Spring 2018

HYDROTREATING TUNGSTEN CATALYST FOR PRODUCTION OF GREEN DIESEL FROM BIODIESEL

Gagandeep Dhillon
University of New Hampshire, Durham

HYDROTREATING TUNGSTEN CATALYST FOR PRODUCTION OF GREEN DIESEL FROM BIODIESEL

BY

GAGANDEEP SINGH DHILLON

B.E., Chemical Engineering, M.S. University of Baroda, 2016.

THESIS

Submitted to the University of New Hampshire in Partial Fulfillment of

the Requirements for the Degree of

Master of Science

in

Chemical Engineering

May 2018

This thesis has been examined and approved in partial fulfillment of the requirements for the degree of Master of Science in Chemical Engineering by:

Thesis Director: Dr. Palligarnai T. Vasudevan
Professor of Chemical Engineering
Senior Vice Provost for Academic Affairs

Dr. Nivedita R. Gupta
Professor of Chemical Engineering

Dr. Nan Yi
Assistant Professor of Chemical Engineering

On December 11th 2017

Original approval signatures are on file with the University of New Hampshire Graduate School.

DEDICATION

I dedicate my thesis to my respected parents, sister and brother-in-law.

ACKNOWLEDGEMENTS

First of all, I would thank GOD for blessing with lot of opportunities and help he has given me. I would like to express my profound appreciation and gratitude to Dr. P. T. Vasudevan, who has provided me guidance and support over the past 2 years as my advisor and mentor for M.S. program. He has been a great source of knowledge and wisdom and I have been truly fortunate to have the opportunity to work with him. Sincere thanks to Dr. Vasudevan and Dr. Carr who provided me research assistantship/grading support, which helped me a lot and always motivated and supported me throughout my M.S. program.

I would also like to appreciate the rest of my thesis committee members, Dr. Gupta and Dr. Yi for their constant help, support and guidance. In addition, I would like to thank Dr. Ye Deng for help training me to work with the experiments. Thanks to instrumentation analyst Darcy Fournier for constant help throughout my research.

Lastly, I would like to recognize my parents, sister and brother-in-law for always being there and believing in me. Once again thanks a lot to everyone.

TABLE OF CONTENTS

LIST OF FIGURES

LIST OF TABLES

ABSTRACT

HYDROTREATING TUNGSTEN CATALYST FOR PRODUCTION OF GREEN DIESEL FROM BIODIESEL

BY

GAGANDEEP SINGH DHILLON

University of New Hampshire, May 2018.

The search for alternatives to petroleum-based fuels has led to the development of fuels from various sources, including renewable feedstocks such as fats and oils. Several types of fuels can be derived from these triacylglycerol-containing feedstocks. One of them is biodiesel, which is defined as the mono-alkyl esters of vegetable oils or animal fats. Biodiesel is produced by transesterifying the oil or fat with an alcohol such as methanol under mild conditions in the presence of a base catalyst. Another kind of product that can be obtained from lipid feedstocks is a fuel whose composition simulates that of petroleum-derived diesel fuel. This fuel termed as ‘‘green diesel’’, is produced from biodiesel by hydrodeoxygenation reaction at elevated temperature and pressure in the presence of a catalyst. Here, tungsten is used as hydrodeoxgenation catalyst to get green diesel from biodiesel. In this research, the effects of feed-stock, reduction and reaction temperatures, hydrogen flowrate and choice of

promoter on the hydrodeoxygenation activity of the catalyst were examined. It is found that reduction and reaction temperatures are the two most important parameters for overall biodiesel conversion and yield of green diesel. The results for unpromoted and promoted tungsten catalyst are compared with the results for both the oxide and sulfide forms of the catalyst.

Chapter 1

INTRODUCTION

Hydrodeoxygenation (HDO), hydrodesulphurization (HDS), hydrodenitrogenation (HDN), hydrodemetallization (HDM) and hydrogenation (HYD) are the main hydrotreating processes that occur simultaneously during hydroprocessing of petroleum feedstocks for the production of fuels. To address the environment problems, removal of sulfur and nitrogen from petroleum feedstocks is necessary because SO_X and NO_X are generated by combustion of fossil fuels. Also, N-compounds in the feed poison catalysts; therefore, their removal is required to achieve deep HDS of fuel in a final hydroprocessing step. During HDO, oxygen in the feed is converted to H_2O which is environment friendly. Some of the O-compounds in the feed readily polymerize and may be the cause of rapid catalyst deactivation thus removal of oxygen is necessary [1]. HDO of biodiesel is fairly recent; biodiesel contains esters of long chain fatty acids (FAME) and removal of oxygen from it produces green diesel with a higher cetane number. Biodiesel fuel can be produced by transesterification of virtually any triglyceride feedstock. This includes oil-bearing crops, animal fats, and algal lipids. The literature contains hundreds of references of biodiesel production from a wide variety of feedstocks [16].

Property	Petroleum Diesel	Biodiesel	Green Diesel
Carbon %	86.8	76.2	84.9
Hydrogen %	13.2	12.6	15.1
Oxygen %	0.0	11.2	0.0
Specific gravity	0.85	0.88	0.78
Cetane Number	40-55	45-55	70-90
Kinematic Viscosity (mm^2/s)	2 – 3	4 – 5	3 – 4
Energy Content (MJ/Kg)	43	39	44

Table 1. Properties of petroleum diesel, biodiesel and green diesel [35].

Triglycerides-based feedstocks such as sunflower oil, coconut oil, jatropha oil, palm oil and rapeseed oil are used for production of biodiesel and green diesel. Relatively cheaper feedstock such as waste cooking oil can also be used [28]. Methyl esters can be hydrogenated to fatty alcohols or hydrolysed to fatty acids. Specific temperature/high pressure and catalysts are required for direct hydrogenation of esters to alcohols. Lewis acid sites of alumina support plays important role in ester hydrolysis. Methyl esters are less prone to hydrolysis than compounds containing β-hydrogen atoms [7].

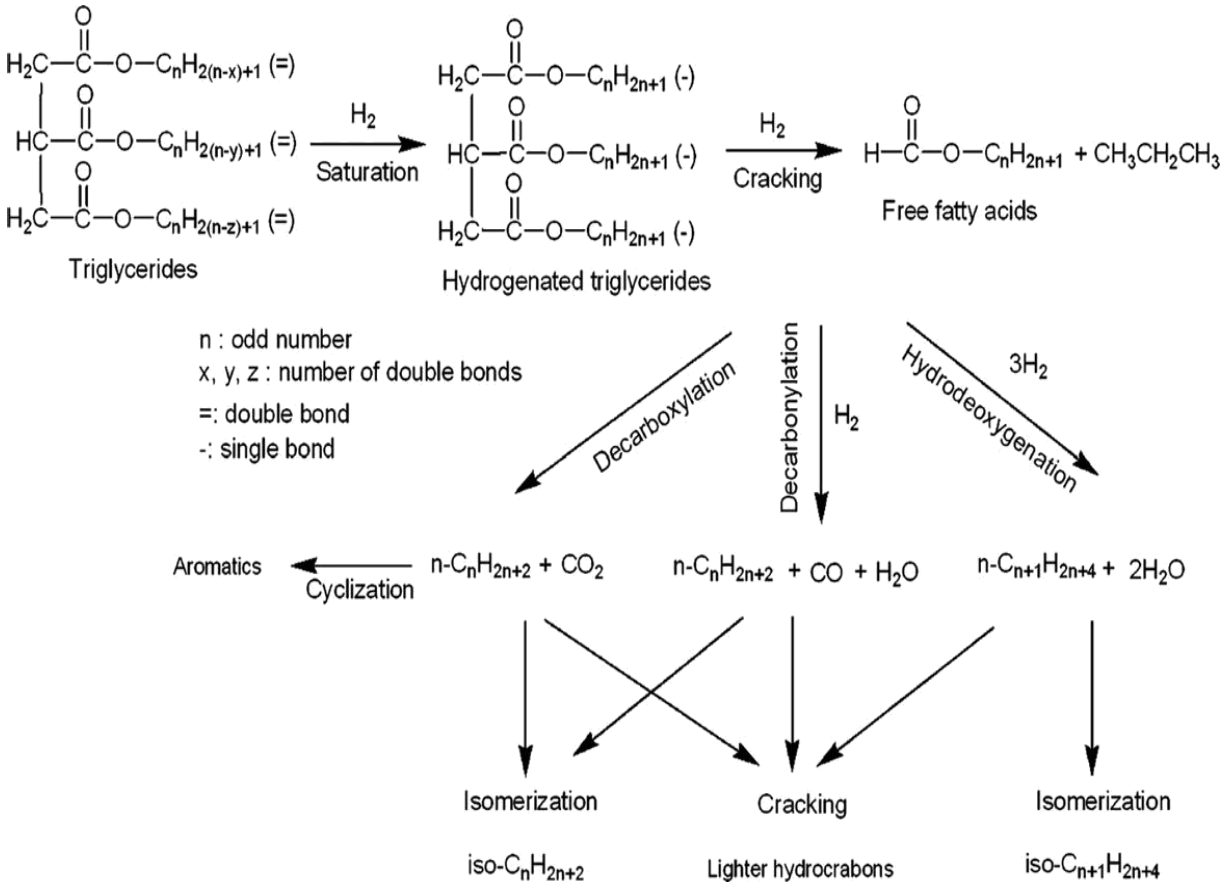

Fig. 1.1 Possible routes of deoxygenation reaction [2].

However, free fatty acid content being high, difficulty arises in production of biodiesel. There are mainly three routes of upgrading triglycerides – 1st is the transesterification with methanol to produce FAME, 2nd is selective deoxygenation to produce green diesel using hydrotreating catalysts such as Ni, Mo, W, Pd, etc. and the 3rd method is hydrocracking using acidic supports. The most common mechanism in the deoxygenation (DO) of triglycerides and biodiesel involves the following steps – first, the saturation of double bonds of the fatty acid chain is followed by the formation of propane and carboxylic acids

via hydrogenolysis and then the formation of hydrocarbons through decarbonylation or decarboxylation or hydrodeoxygenation in which CO, CO_2 or H_2O is removed as by product respectively [28]. The commonly used hydrodeoxygenation catalysts are supported noble and sulfided or oxided metal catalysts. Co-Mo/Al_2O_3, Ni-Mo/Al_2O_3 and W-Ni/Al_2O_3 are widely used for hydrodeoxygenation [2]. Intensive research in the last decade has shown that palladium based and bimetallic NiMo, CoMo and NiW catalysts supported on high surface area supports are promising choices for selective deoxygenation of natural triglycerides and FAME to produce green diesel [28]. Noble metals supported on various high surface carriers and conventional NiMo, CoMo and NiW sulfided catalysts have been proven to be very promising for upgrading of petroleum feedstocks and hydrotreating reactions. However, the noble metal catalysts seem to be not viable economically. This is due to their limited availability and high cost. Also, they may seem to be contaminated by oxygenated compounds present in the feedstock [20]. Many factors that affect the HDO activity are: presence of water and ammonia, support materials, sulfidation temperature, H_2S partial pressure, loading of metal and impregnation order. Those of tungsten-based catalysts are strongly dependent on degree of sulfidation. WS_2 is formed via oxysulfide (WOS_2) intermediate from WO_3. With increase in calcination temperature, the sulfidability of tungsten degrades which is related to degree of interaction between tungsten species and support materials. As interaction of tungsten with titania support being less, sulfidation is facilitated over W/TiO_2 catalyst but with alumina support, its interaction is stronger and thus sulfidation decreases with increase in calcination temperature [9].

Organometallic catalysts are reported to be highly reactive and reaction specific thereby minimizing side reactions so their continuous useability is less and thereby losing its

acidity in the long runs. Same is the case with fluoride modified NiMo catalyst [14]. Sulfided catalysts are considerably more active than the corresponding reduced ones when the conventional Co(Ni)Mo(W)/γ-Al_2O_3 is compared with its counterparts in reduced form and sulfided form. An effort has been recently undertaken to develop Co(Ni)-Mo(W) / γ -Al_2O_3 reduced catalysts with higher activities similar to those of the corresponding sulfided ones. This was done by doping the support with lanthana, ceria and phosphorous. The resulting catalysts showed similar catalytic activity as corresponding to non-doped sulfided ones [21]. The catalytic synergy between Ni(Co)Mo(W)/Al_2O_3 catalysts is due to formation of NiMoWS or CoMoS phases where highly dispersed $MoWS_2$ crystallites are promoted by Ni or Co [29]. The active phase Co(Ni)-Mo/S is dispersed by the presence of γ-alumina support in hydrotreating reactions. Fully sulfided catalysts results in most active catalysts. On the other hand, some interaction between Mo and the support is usually assumed to be beneficial for high MoS_2 dispersion. It has been shown that sulfided CoMo and NiMo catalysts supported on activated carbon in HDS reactions gives outstanding performances due to their weak interaction with the active metal sulphides [23]. The Sulfided NiMo/γ-Al_2O_3 catalyst exhibited high rate of isomerized product activities due to high acidity of the catalyst thus giving high HDO rates and selectivities. Iso paraffins are more important than normal ones due to their cold flow properties such as cold flow filter point and freezing point of biofuel. Addition of urea in Ni and Mo organometallic complexes improves the metals' dispersion and solubility in the γ-Al_2O_3 support which in turn enhances its morphology and textural properties leading to the formation of highly reactive octahedral molybdenum and nickel oxides with proper acidity [14].

In hydrotreating reactions, alumina is mostly used as support due to its high thermal stability and higher surface area. But it suffers coke formation on its surface due to its strong interaction with the metal oxide thus hindering its sulfidation and this is due to presence of acid sites on alumina surface. As compared to this, carbon is more preferable than alumina due to its surface inertness and amphoteric properties. Also, carbon supports stabilize CoMoS active phase [15]. So, by combining the properties of carbon and alumina is an interesting way to overcome the demerits of alumina support. Incorporating carbon in alumina results in decrease in interaction between support phase and sulfide phase of catalyst. Titania is preferred over alumina and carbon support on MoS_2 catalyst in HDO reactions. For CoMoS systems, zirconia as a support offers highest activity to the catalyst [10]. However, industrial application of carbon supports is limited due to its low packing density and small porosity. In HDS of vacuum gas oil blended with 15% of sunflower oil over Co-PMo/Al_2O_3 catalyst, there is increase in cetane number by 5 and this is due to conversion of fatty acid triglycerides to linear alkanes thus increasing pour point of hydrogenated products by 5 ºC [15].

Silica supported metal phosphides are also very active for HDO reactions and those prepared from phosphite precursors have high surface area along with good catalytic activity. Also, transition metal phosphides of Ni, Mo, W and Fe are highly active for HDS and HDN of petroleum feedstocks. Regarding the supports, less acidic materials such as silica, hexagonal mesoporous silica and MCM-41 favour the formation of metal phosphides due to low interaction between support and precursor which is usually metal phosphate or metal phosphite. As phosphites and hypophosphites are low in their oxidation states, they are more easily reducible at lower temperatures as compared to phosphate precursors. Of

all aforementioned catalysts for hydrotreating reactions, Ni_2P prepared by phosphate precursor is the most effective catalyst [27].

In this study of HDO reactions, we used tungsten oxide (WO_3) and tungsten sulfide (WS_2) along-with Ni promoted tungsten oxide and tungsten sulfide catalysts supported on γ-Al_2O_3. The supported tungsten oxide catalysts find numerous applications like hydrocarbon cracking, hydrodesulfurization, hydrodenitrogenation, hydrodeoxygenation, olefin metathesis, alkane isomerisation and selective catalytic reduction. [4]. Supported oxides and sulfides of molybdenum and tungsten are well known for catalyzing a great variety of reactions. W-based catalysts have been reported to have better properties than Mo-based catalysts [12].

The broad objectives of this thesis are as follows:

1. To prepare supported tungsten oxide by decomposition of ammonium metatungstate and tungsten sulfide by decomposition of ammonium tetrathio-tungstate in hydrogen; to prepare Ni promoted oxide and sulfide catalysts and to compare the activity of both catalysts.
2. To study the effect of various pretreatment and reaction temperatures on the overall conversion, yield and selectivity.

This thesis is divided into five chapters. Chapter 2 contains literature review on different catalysts employed for hydrodeoxygenation and its mechanism. Chapter 3 describes the experimental setup and procedures for making catalysts and reaction runs. Chapter 4 presents the results of the study and lastly the conclusions and recommendations are presented in Chapter 5.

CHAPTER 2

LITERATURE REVIEW

2.1 Hydrodeoxygenation general mechanism

The main route in the formation of hydrocarbons (C_{11}-C_{18}) from fatty acid methyl esters ranging from methyl laurate to methyl oleate involve decarbonylation or/and decarboxylation which proceeds by hydrogenation of unsaturated C=C bonds, progressive hydrogenolysis of the C=O bond to fatty acid and finally reduction to lead hydrocarbons via intermediate aldehyde formation. The second route in C_{11}-C_{18} hydrocarbons formation is known as hydrodeoxygenation involves aforementioned steps leading to formation of intermediate alcohols by dehydration on acid sites and then hydrogenation on active metal sites to produce hydrocarbons [3, 20, 28].

2.2 Ni catalysts for HDO

Jenistova et al. [13] have investigated HDO of stearic acid and tall oil fatty acids using Ni catalyst supported over γ-Al_2O_3. They studied the effect of pressure on the HDO activity of Ni/γ-Al_2O_3 at a reaction temperature of 300 ºC. Low metal loaded catalyst (5%) was prepared and during H_2-TPR, it was found that NiO species are reduced to Ni^{2+} which attributed to octahedral position. HDO of stearic acid over Ni/γ-Al_2O_3 which was reduced at 450 ºC ex-situ in absence of hydrogen atmosphere revealed very low conversion of stearic acid (19%) and low selectivity to C_{17} alkanes (26%). By carrying out reaction in hydrogen atmosphere, the conversion was increased from 19% to 80%. This necessitates the requirement

of hydrogen in HDO reactions. Also, necessity of pre-reduction was studied and it was found that pre-reduced catalyst had overall conversion of 99% vs 31% obtained with unreduced catalyst. Moreover, unreduced catalyst had 84% selectivity towards C_{17} while remaining as stearyl alcohol whereas reduced catalyst had 97% selectivity to C_{17} hydrocarbon. Possible explanation for this can be redispersion of Ni particles on the support and formation of smaller Ni particles during in-situ reduction.

Previous studies on HDO of stearic acid over 15 wt% Ni/γ-Al_2O_3 reveals first order kinetics based on power law model and apparent activation energy is found to be 175.4 kJ/mol which is greater than FeMoOx/zeolite catalysts for which HDO activation energy is about 130.3 kJ/mol. Precious metal-based catalysts were found to be more effective in lowering activation energy than the base metal catalysts. The apparent activation energy of HDO of palm stearic fatty acid mixture over 5% Ru/Al_2O_3 was reported to be 49.22 kJ/mol, with the order of 0.8 with respect to H_2 partial pressure and 1.2 to liquid reactant [22].

Hong et al. [9] studied hydrodeoxygenation of guaiacol over NiW/TiO_2 at a reaction temperature of 300 ºC and hydrogen pressure of 7 MPa for 150 min and they found that products were mostly cyclohexane and benzene with some amounts of phenol, anisole, catechol and cresol with 100% conversion and 16% yield of cyclohexane. NiW/TiO_2 proved to be best catalyst among Co promoted and commercial catalyst. Moreover, it was found that Co didn't promote the catalyst as Ni promoted.

Ayodele et al. [14] studied hydrodeoxygenation of oleic acid into normal and iso-octadecane using Ni oxalate catalyst supported on alumina. This group reported that as catalyst loading increased from 10 mg to 30 mg, there is an increase in the HDO activity of the catalyst due to increase in the active Ni sites for the reaction. By formation of n-C_{18} due to HDO of

oleic acid, there was formation of iso-C_{18} which is a secondary reaction. The catalyst was reduced at 200 ºC *in-situ* for 1 h prior to reaction. As the reaction temperature increased from 320 ºC to 360 ºC, the yield of n-C_{18} increased from 40% to 72% and yield of iso-C_{18} increased from 5% to 21%. Moreover, on increasing the reaction temperature to 360 ºC, the ratio of iso-C_{18} to n-C_{18} increased, which implies that secondary reactions are more dominant at higher reaction temperatures.

Sulfur free Ni catalyst have been studied for production of green diesel by HDO over Ni catalyst. Hachemi et al. [16] used γ-Al_2O_3, SiO_2 and H-Y zeolite as support materials and quite interesting results were found. Transformation of stearic acid was more rapid over Ni/H-Y than over Ni/Al_2O_3 and Ni/SiO_2, giving respective conversions values after 90 min of 94%, 43%, and 46%. Here, stearyl alcohol appeared as an intermediate in the first 2 h of the reaction and then disappeared completely at the end of the reaction. Nickel supported on nonacidic activated carbon gives high selectivity to C_{17} HCs through decarboxylation of stearic acid. High selectivity to C_{18} HCs can be inferred from the fact that high acidity of the supports leads to sequential hydrogenation of fatty acids to aldehydes and alcohols on nickel metal clusters followed by dehydration of fatty alcohols on Bronsted acid sites to olefins and hydrogenation of the double bond on the metal. The catalyst deactivated after the 1st run showing 39% decrease in surface area for Ni. Another reason for catalyst deactivation is the decrease in the pore size and thereby decreasing the number of active sites. Also, minor increase in the metal size led to reduction in the reaction rates. The zeolite-containing catalysts tend to become deactivated and are generally regenerated at high temperature with oxygen containing gas to restore their activity.

Gousi et al. [20] studied Ni-alumina co-precipitated catalysts. The reaction products mainly consisted of normal HCs in the diesel range (C_{15}-C_{18}), fatty acids and unreacted triglycerides. Propane, ethane, CH_4, CO, and CO_2 were detected in the gas phase indicating decarbonation to be dominant reaction route over hydrodeoxygenation on Ni/Al_2O_3 catalysts. The total yield to hydrocarbons increased with the nickel loading up to the sample 60NiAl and then it decreased. The initial increase in Ni loading led to increase in the HC production and then it decreased due to amount of $NiAl_2O_4$ like phase present on the catalyst surface which seems to be difficult to reduce even at 700 ºC and thus inactive for hydrogen transfer reactions. Complete conversion of sunflower oil into hydrocarbons in the diesel range was achieved after 3 h. the product distribution was: 86% C_{17}, 4% C_{18}, 9% C_{15} and 1% C_{16}. The heating value of this product was calculated to be almost equal to 43.9 MJ/kg, which is very close to the heating value of diesel (43.4 MJ/Kg). Mild acidity promotes selective deoxygenation and prevents extensive cracking. Catalyst prepared by controlled co-precipitation/activation method resulted in nickel-alumina nano-structured mesoporous material having very high surface area thus giving high catalytic activity.

2.3 Mo catalysts for HDO

Hydrodeoxygenation of oleic acid into n- and iso- paraffin biofuel using zeolite supported fluoro-oxalate modified molybdenum catalyst have been studied [6]. This research reports that HDO of oleic acid proceeds by hydrogenation to stearic acid and then subsequent deoxygenation to produce n- and iso- C_{18}. At the end of 60 min of reaction, 59% of n- C_{18} and 21% of iso- C_{18} was found in the reaction product along-with stearic acid and traces of gases. Increasing the loading of catalyst and the reaction temperature also increased the yield of iso-

C_{18} as compared to n-C_{18}. Also, the rate of reaction of hydrogenation of oleic acid to stearic acid was higher than deoxygenation that implied deoxygenation to be rate controlling step in HDO process. The catalyst didn't deactivate after its reusability over 3 consecutive experiments and this is due to formation of fluoro-molybdenum-oxalate complex. Due to strong carbon-fluorine chemical bond, the corresponding fluoro-metal-oxalates have been reported to have very high thermal and chemical stability. Higher dispersion of Mo species on the support caused by the functionalization of flouride and oxalate makes them highly reactive octahedral catalysts that are superior than conventional tetrahedral Mo oxide catalysts. Here, the formation of iso-paraffin (C_{18}) was thought to be because of increased acidity due to oxalic acid functionalization. Also, isomerised compounds are value added ones due to their lower freezing point and their applications for cold flow properties. One US patent claim that metal-oxalate catalysts are reaction specific thus minimizing side products. Research by Deng [17] showed that Mo has C_{18}/C_{17} ratio between 10-13 and conversion about 59% for HDO of methyl oleate and biodiesel, which indicates that Mo favours hydrodeoxygenation over decarbonation to produce diesel ranged products.

2.4 Ni-Mo catalysts for HDO

Hydrodeoxygenation of methyl oleate over sulfided Ni-Mo catalysts has been studied by Coumans et al [23]. It is demonstrated that NiMo/Al_2O_3 and NiMo/ASA (amorphous silica-alumina) are very active during their early hours of operation but their activity decreases with time. Higher initial activity of NiMo/Al_2O_3 and NiMo/ASA is supposed due to presence of Al^{3+} sites on the Al-containing support surfaces. Deposition of FAMEs on the support block these Al^{3+} sites and slows the rate of methyl ester hydrolysis. Thus, alumina and ASA

supported catalysts exhibit deactivation after prolonged use. Also, NiMo/C has higher activity, C_{17}/C_{18} selectivity and yield as compared to $NiMo/SiO_2$ catalyst and this can be due to an intrinsically higher activity of the metal sulfide phase in this HDO reaction.

Wang et al. [24] investigated the effect of feedstock on the product distribution using 5%Ni-10%Mo supported over γ-Al_2O_3. HDO of waste cooking oil and algal oil over 5%Ni-10%Mo/γ-Al_2O_3 yields 74.48% and 62.57% HCs respectively. The low reactivity is mainly attributed to the presence of an excess larger molecules such as diaclyglyerols and triacylglycerols in waste cooking oil and algal oil. HDO efficiency increases with increase in Mo loading (5% to 10%) from 92.3% to 96.7%. Further increase in loading upto 30% doesn't affect efficiency much giving increase of only 0.3% in conversion. Increase in Ni loading from 3% to 7% doesn't affects the HDO efficiency and remains nearly same (~97%). But product distribution is affected by Ni loading. On higher Ni loadings, linear alkanes dominate the reaction products while branched alkanes are less formed whereas low Ni loading enhances the formation of branched alkanes, cycloparaffins, alkyl benzenes and linear alkanes. The 5%Ni-10%Mo catalyst proved to be most stable for HDO reactions upto 120 h. also, the HDO yield remained constant (~97%) during this time.

Coumans et al. [7] studied the hydrodeoxygenation of oleic acid, methyl oleate and triolein over alumina supported NiMo sulfide. During HDO of methyl oleate, fatty acids (oleic acid), along with aldehydes and alcohols are found to be the reaction intermediates that produces C_{17} and C_{18} hydrocarbons. Methane is found to be dominant reaction by-product with traces of CO and CO_2 indicating that CO and CO_2 are methanated under reaction conditions. The HDO reaction carried out at 260 ºC and 60 bar exhibited 1^{st} order reaction and –0.09 with respect to H_2S and activation energy of 193 kJ/mol. Also, for methyl heptanoate, the rate of

decarbonation is found to be increasing with increase in H_2S on NiMoS/γ-Al_2O_3. Hence its can be said that decarbonation is promoted by H_2S and HDO is inhibited by H_2S. Also, along with C_{17} and C_{18} alkanes, some amount of olefins (α-olefins) are also formed during decarbonation of methyl oleate. MoS_2 is found to be more selective for HDO than decarbonation. Selectivity of olefins increases with time and with deactivation of catalyst, decarbonation was less affected by deactivation while HDO was more affected. Due to blocking of Lewis acid sites of alumina support, the catalyst gets slowly deactivated with time thus decreasing the rate of hydrodeoxygenation. Kinetics of HDO of triolein and methyl oleate were found to be similar. If alkali metals are present as minor impurities in the catalyst, then it can deactivate the catalyst.

Hydrodeoxygenation of oleic acid was investigated by Ayodele et al. [18] using Mo modified zeolite supported Ni oxalate catalyst functionalized with fluoride ion. Increase in process parameters such as temperature, pressure and catalyst loading lead to increase in normal paraffins from 40% to 73% and iso-paraffins from 10 to 23%. Best conversions and yields were observed at 360 ºC and 20 bar pressure and catalyst loading of 30 mg. The presence of iso paraffins was due to the functionalization of catalyst with fluoride ion. The catalyst reusability showed marginal loss of 2% after 3rd use.

Hydrodeoxygenation of methyl laurate was studied [19] over supported Ni-Mo catalysts under low hydrogen pressure. The catalyst was pre-reduced under hydrogen at 370ºC and then HDO was carried out at 300 ºC and 0.4 MPa pressure and LHSV of 40 h^{-1}. This research showed that γ-Al_2O_3 didn't catalyze the reaction and conversion was about 0.1% only. Introducing Ni species on γ-alumina support enhanced the reaction rate thereby giving conversion values upto 30%, 55% and 80% when loading was 10wt%, 20wt% and 28wt%

respectively. Also, yield of undecane increased with increasing Ni content which indicated its high dependency on Ni content. The yields of lower hydrocarbons (C_2-C_{10}) was also increased. But in contrast to this, yield of dodecane didn't had any significant change to Ni content, rather it was formed in very negligible amount indicating decarbonylation and decarboxylation to be controlling mechanisms. Also, formed CO and CO_2 were readily converted into CH_4, - which implies that Ni species also readily catalyse methanation of CO_2 and CO. The hydroconversion using NiMo/γ-Al_2O_3 catalyst was higher than their individual sum of conversions. Moreover, phosphorized Ni catalysts had lower activity even though using higher hydrogen pressure of about 3 MPa. NiMo exhibited smaller yield ratios of C_{11}/C_{12} as compared to Ni and Mo over γ-alumina, which is similar to ratios observed over sulfided NiMo catalysts for hydroconversion of triglycerides. By addition of Mo, catalytic activity of Ni/Al_2O_3 was improved and yield of C_2-C_{10} HCs decreased. These observations suggest synergistic effect between Ni and Mo species even without the sulfurization to play important roles in improving in the catalytic activity, accelerating the HDO reaction, and suppressing the hydrocracking of the hydrocarbon products as well as the methanation of CO.

Synergistic ratio of the NiMo/γ-alumina reduced catalysts have been investigated by Kordoulia et al. [21] for the transformation of natural triglycerides into green diesel. Maximum yield is observed for Ni/Ni+Mo ratio of about 0.8, i.e. 3.5Ni0.5Mo. The reduced catalyst 1Ni3Mo with Ni/Ni+Mo atomic ratio of 0.25 showed very less yield to hydrocarbons (~3% and 39% conversion) compared to sulfided catalysts NiMo having same atomic ratios (0.25) which showed 94% conversion of sunflower oil and 21% yield to diesel range HCs thus proving sulfided catalysts to be more superior than reduced ones for

hydrotreating applications. The critical synergistic ratio is similar for HDS and SDO for the NiMo/ γ-Al_2O_3 catalysts in their sulfided form (about 0.3) but this ratio is very different for the SDO concerning the reduced form of the catalysts (about 0.8). Explanation for this is that the active sites in the sulfided phase are located at MoS_2 slabs decorated by nickel ions (NiMoS phase) whereas the active sites in the reduced state are metallic nickel atoms promoted by MoO_3 or MoOx (with Mo oxidation number between 5 and 4).

A review paper [11] reported that DO of rapeseed oil at reaction conditions of 240 ºC – 280 ºC 35 bar and 0.25 – 4 h^{-1}over sulfided NiMo catalysts supported on alumina mainly produced saturated HCs with even number of carbon atoms. The triglycerides first saturated and then converted into fatty acids which underwent further hydrogenation to yield fatty alcohols and then hydrocarbons. In the DO of rapeseed oil, NiMo/Al_2O_3 catalyst exhibited higher HC conversion, selectivity and lowest catalytic deactivation as compared to Ni/Al_2O_3 and Mo/Al_2O_3. Further, NiMo resulted in both HDO and DCX while Mo favored only HDO and Ni formed only DCX products. HDO reaction of low-grade waste cooking oils and trapped grease over NiMo sulfided catalysts supported on alumina and solic acid (B_2O_3-Al_2O_3) reported higher HDO activity with minimum olefin formation. DO of unsaturated feedstocks under Ar/He atmosphere instead of H_2 causes undesired reactions like cracking and formation of heavier products. So, it can be concluded that H_2 assisted environment is best for carrying out DO reactions.

Gutierrez et al. [5] studied role of sulfur-containing groups in the reaction network in the HDO of model compounds using NiMo/γ-Al_2O_3. The reactions were carried out between 200 ºC – 360 ºC temperature and 1.5 – 8 MPa. Sulfur containing groups on the catalyst surface after presulfiding forms the basis for HDO scheme. The introduction of nucleophile SH^- is the

primary factor in activation of the starting compounds. Adding H_2S improved the reactivity of methyl heptanoate and guaiacol but decreased for phenol and also addition of H_2S lead to shifting the selectivity from C_7 HCs (formed without adding H_2S) to C_6 HCs. The sulfided catalysts show Bronsted acid character because SH^- exists on the surface of the catalyst. From this research, it was found that NiMo is more active than CoMo catalyst providing higher hydrogenation activity, conversions and selectivity. Water as an additive also had profound effects on conversions and product selectivities. It was found that with increasing the amount of water, C_7 HCs formation increased over C_6 and conversion was lowered. Addition of H_2S together with water recovered the activity but formation of C_6 HCs increased.

2.5 CoMo catalysts for HDO

Nikulshin et al. [10] investigated use of carbon-coated alumina as support over CoMoS catalyst for hydrodeoxygenation of oleic acid and guaiacol. The reaction rates of both guaiacol and oleic acid followed pseudo 1^{st} order kinetics. Reactions were carried out between 260 ºC – 340 ºC, 3.0 MPa hydrogen, 12-80h^{-1} LHSV. The guaiacol conversions varied from 32 % to 60% and HDO degree was between 13%-22% at 260°C. Maximal conversions were achieved over $CoMoS/C_2/Al_2O_3$ catalyst. Two routes were dominant in HDO of guaiacol: by methylation with formation of catechol and its derivatives and methane (major route) 2) and through demethoxylation with formation of phenol and methanol. phenol was major product over all catalysts. With increase in reaction temperature to 340 ºC, the guaiacol conversion reached upto 96% over all types of catalysts. The activation energy is reported to be 67-71 kJ/mol. Deactivation degree in guaiacol conversion and HDO decreased from 46% to 31% and from 69% to 4% respectively with increase of carbon content in the C_x/Al_2O_3. Oleic acid:

the conversion of oleic acid varied from 41% to 57% and the HDO degree was 33% - 53%. Rate constants in oleic acid were 3-7 times higher than in guaiacol. C_{17} and C_{18} HCs were the main reaction products in the HDO of oleic acid. Also, there were minor amounts of shorted fatty acids and C_{18} aldehydes and alcohols. Approaching the reaction temperature of 340 ºC, the oleic acid conversion reached 80% - 100% and activation energy was found to be 64 - 66 kJ/mol. Deactivation degrees in oleic acid conversion and HDO decreased from 31% to 2% and from 29% to 1% with increase in carbon content in C_x/Al_2O_3 supports upto 5.6 wt% of carbon. The catalyst deactivation due to formation of coke was attributed to Lewis acid-base pairs on the alumina. So, by adjusting the acidity of the alumina, effective HDO catalysts could be designed.

2.6 Pd catalysts for HDO

Stearic acid hydrogenation was studied [26] over Pd nanoparticles embedded in mesoporous hypercrosslinked polystyrene and it was revealed that the use of 1% Pd/HPS allowed converting stearic acid upto 97% heptadecane yield. The conversion increased from 15% to 97.5% when the temperature was increased from 230 ºC to 300 ºC at a constant pressure of 0.6 MPa. Also, increase in pressure from 0.2 MPa to 1.8 MPa increased the conversion from 55% to almost 100% when the temperature was constant (255 ºC).

On Pd catalysts supported on carbon, decarbonylation and decarboxylation were the main routes of deoxygenation of stearic acid with products mainly dominated by C_{17}s Moreover, C_{17}s were also products when oleic acid was deoxygenated with Pd/C as catalyst. Also, with Carbon supported Ni and Pt catalyst, the major products C_{17}s as in the case of Pd/C. Highest activity was observed with Pd/C catalyst. During DO of ethyl stearate

over Pd catalysts, nearly double reaction rate was observed when reaction temp increased from 300 ºC to 330 ºC. Deoxygenation tendency of catalysts increases with higher metal loading and this is attributed to higher number of active sites on the catalyst surface thus increasing formation of diesel ranged products [11]. Pd/Al_2O_3 showed an increase in the conversion from 0.4% to 5% in HDO of 2-methyl tetrahydrofuran when temperature was raised from 250 ºC to 350 ºC. This is anticipated due to carbon deposition on the catalyst surface thus blocking the active sites for the reaction and resulting in low conversion [27].

2.7 Pt catalysts for HDO

Zhou et al [22] studied the kinetics of hydrodeoxygenation of microalgal oil over Pt/ γ-Al_2O_3. Kinetic study of microalgal oil over 1% Pt/γ-Al_2O_3 revealed activation energy about 60.3 kJ/mol considering power law and eley-rideal mechanism of adsorption which is lower than the intrinsic activation energy of 92.9 kJ/mol obtained considering langmuir-hinshelwood kinetics which is assumed due to the exothermic adsorption of reactants. Also, H_2 was found to be adsorbed on the surface without dissociation which is different from gaseous reaction with consistent dissociative adsorption of H_2. The rhenium-modified Pt/H-ZSM-5 catalyst showed superior catalytic activity and excellent HC conversion towards C_{15}-C_{18} compared to Pt/H-ZSM-5 for hydrotreating of jatropha oil [11].

2.8 Fe catalysts for HDO

MSN-supported iron nanoparticles have been investigated by Kandel for HDO of microalgal oil et al [25]. C_{18} was the major reaction product after 6 h of reaction (yield ~87%) while C_{17} was a minor product (yield~12%) indicating hydrodeoxygenation to be the most dominating reaction pathway. In contrast to hydrogenation of oleic acid over MSN supported Ni catalysts mostly produced cracking products with very low selectivity towards diesel range products. Stearic acid and octadecanol were the major reaction intermediates during the course of reaction. Octadecanol disappeared slowly as compared to stearic acid implying hydrodeoxygenation to be more dominant that decarbonation mechanisms. Aldehyde was not detected under the reaction conditions indicating aldehyde reduction rate was fast over Fe-MSN catalysts. The production of HCs increased dramatically (conversion ~100%) from 230 ºC to 290 ºC with major increase in formation of octadecane while hydrocracking and decarbonylation was not observed until 290ºC. This implies that activation energies for cracking and decarbonation is higher as compared to hydrodeoxygenation reaction over Fe-MSN catalysts. Low hydrogen pressure (10 bar) favoured decarboxylation, decarbonylation and cracking while high hydrogen pressures (40 bar) favoured hydrodeoxygenation. As Fe forms strong metal-oxygen bond than Ni, hydrodeoxygenation is favoured over decarbonation by stopping the reaction at decarbonyl stage due to high retention time of the oxygenated compound on the catalyst surface.

2.9 Rh catalysts for HDO

Bie et al. [3] reported HDO of methyl palmitate over bifunctional Rh/ZrO_2 at a reaction temperature of 270 ºC and 80 bar pressure. In this project, pentadecane was the dominant reaction product along with a little hexadecane. The concentrations of palmitic acid and hexadecanol was also found to decrease with time indicating their nature as intermediates. The most active sites for the reaction was supposed to be interface between the Rh atoms and the support ZrO_2. Here both the Rh sites and oxygen vacant ZrO_2 sites contribute synergistically for the reaction. Most active catalyst is supposed to be the bifunctional comprising of reducible metal oxide as support and active metal center (noble/transition metal). ZrO_2 supported Pt and Rh catalyst was investigated for HDO of methyl heptanoate and it was found that Rh catalyst had higher activity that Pt catalyst. ZrO_2 manifests an ability to activate oxygenates whereas the presence of metal is responsible for higher activity and hydrocarbon formation. It is reported that decarbonylation and decarboxylation take place over noble metal carbides. (Rh/C and Pd/C). ZrO_2 supported catalysts are found to be more active than C, Al_2O_3 and SiO_2 supports. Oxygen vacancy sites on supports are considered to be active sites for activating carboxylate group of FAME thus forming a ketene species via aldehyde intermediate. It has been found that fatty esters having different HC chain length exhibit different kinetic behaviour.

2.10 Transition metal phosphides as catalysts for HDO

Transition metal phosphides have been studied for hydrodeoxygenation of biofuel model compound by Bui et al [27]. They prepared phosphide catalysts using either phosphites or phosphates as the catalyst precursors. In the HDO of 2-methyltetrahydrofuran, Ni_2P and CoP is selective towards C_4 and C_5 alkanes while WP, MoP and FeP had mostly unsaturated products (pentenes and pentadienes). C_4 is mainly produced through decarbonylation mechanism for which Ni, Co and W are known to be very active. WP/SiO_2 prepared by phosphate method produced pentadienes prior to pentenes, so surface intermediate is suggested to have bound to two active sites for simultaneous dehydrogenation for the initial pentadienes formation whereas WP/SiO_2 prepared using phosphite precursor produces pentenes prior to pentadienes suggesting dehydrogenation to have been occured on a single site. CoP and MoP prepared using phosphite method are more active than phosphate ones while phosphides of W, Ni and Fe prepared using phosphate precursor are more effective than phosphite method. The order of activity of the catalysts prepared by phospite method is WP > Ni_2P > MoP > CoP > FeP and that prepared by phosphate method is Ni_2P > WP > MoP > CoP > FeP. Supported Ni_2P, WP and MoP catalysts show high conversion (~90% – 100%) within the temperatures range of 250 ºC – 350 ºC whereas, FeP prepared from phosphite precursor doesn't show any activity at 275 ºC, and slowly deactivated at 350 ºC [27]. In the SDO of lauric acid, Ni phosphide catalyst mainly produced C_{11} and C_{12} alkanes. The order of catalytic activity of Ni_2P over various supports for high conversion of methyl laurate at 340 ºC. Ni_2P/SiO_2 > Ni_3P-$Ni_{12}P_5/Al_2O_3$ > Ni_2P/TiO_2 > Ni_2P/SAPO-11 > Ni_2P-$Ni_{12}P_5$/HY > Ni_2P/CeO_2. [28].

2.11 Effect of different supports, additives, catalyst to oil ratio and catalyst particle size on HDO [28].

a) Supports.

High acidity of support favours fragmentation while low acidity offers low catalytic activity hence medium-carefully regulated acidity should be best for high yields of green diesel. For zeolite type of supports, relatively high Si/Al ratio leads to low acid site concentration on the catalytic surface. For instance, in the SDO of stearic acid over 10%Ni/HZSM-5 (Si/Al = 45) catalyst, full conversion but severe cracking of hydrocarbon chain was seen and selectivity to green diesel was about 43% only. By using same support with high Si/Al ratio (120 – 200), the acidity decreased leading to higher selectivities to green diesel (84% – 93%). Ni catalysts supported on zirconia, titania and ceria showed almost full conversion for stearic acid with 87 – 96% yield of heptadecane while rest being C_{13}-C_{18} HCs. The high activities of the catalysts on the slightly reducible supports were attributed to the participation of the support surface on the reaction mechanism through defect oxygen sites. Give below is the comparison of Ni, Pt and Pd catalysts on various supports for SDO of palmitic acid.

15%Ni / ZrO_2 = 5%Ni / HZSM-5 (Si/Al = 200) > 5%Ni / HBEA (Si/Al = 180) > 10%Ni/ZrO_2 > 5%Ni / ZrO_2 > 5%Pd / ZrO_2 > 5%Pt / ZrO_2 > 3%Ni / ZrO_2 > 5%Ni / Al_2O_3 > 5%Ni / SiO_2 > 5%Pt / C > 5%Pd / C.

Thus, it seems that zirconia is better support than alumina, silica and activated carbon.

For SDO of methyl palmitate, silica support proved to be least effective while HZM-5 and HY support offered 90% conversion but product distribution was shifted towards lower alkanes rather than diesel ones. The most promising catalyst proved to be 7%Ni /γ-Al_2O_3

and 7%Ni / SAPO-11 which showed high conversion of MP and high selectivity for C_{15} and C_{16}. The good catalytic activity of HZSM-5 and SAPO-11 was attributed to the medium acidity. For SDO of palm oil, 9%Ni / SAPO-11 had almost 83% selectivity to isomerized hydrocarbons indicating good balance between Ni and SAPO-11. Highest selectivity for heptadecane was obtained over Ni / ZrO_2-CeO_2 catalyst for SDO of biodiesel indicating incorporation of zirconia in the support suppresses hydrocracking and favours decarbonation. Most promising supports among the non-reducible oxides are HBeta, SAPO-11, Al-SBA-15 and γ-Al_2O_3 which exhibit high surface area and prevents hydrocracking. In the SDO of lauric acid, Ni phosphide catalyst mainly produced C_{11} and C_{12} alkanes. Given below is the order of catalytic activity of Ni_2P over various supports for high conversion of methyl laurate at 340 ºC. Ni_2P/SiO_2 > Ni_3P-$Ni_{12}P_5/Al_2O_3$ > Ni_2P/TiO_2 > Ni_2P/SAPO-11 > Ni_2P-$Ni_{12}P_5$/HY > Ni_2P/CeO_2.

b) Effect of additives.

SDO of jatropha oil into green diesel over NiMo catalysts supported on alumina doped with lanthana has been studied. 5% Lanthanum doped catalyst (5%Ni10%Mo) is proven to be most promising among non-sulfided catalysts giving maximum yield between 280 ºC – 370 ºC and HC distribution is C_{15} – C_{18}. The well dispersed lanthanum oxide on catalyst promotes the reduction of Ni^{2+} to metallic Nickel while it also oxidizes Mo^{4+} to Mo^{6+}. Moreover, lanthanum oxide increases the basicity of the catalyst. Similar characteristics are observed in NiMo catalyst when cerium oxide is doped into it. Most active catalyst is 5% Ceria doped non sulfided NiMo/Al_2O_3. Also, these non-sulfided catalysts have been found to be equivalent to the corresponding sulfided ones in their action. In SDO of biodiesel over Ni and Ni-Cu catalysts, absence of CO and CO_2 formed as a result

of decarbonation confirms that methanation also takes place consuming more hydrogen in the process.

c) Effect of catalyst to oil ratio.

For SDO of soybean oil, the conversion is dependent on catalyst to oil ratio. When the ratio was 0.044 the following order was obtained. NiMo/γ-Al_2O_3 (92.9%) > 5%Pd / γ-Al_2O_3 (91.9%) > sulfided CoMo / γ-Al_2O_3 (78.9%) > 66%Ni / SiO_2-Al_2O_3 (60.8%) > 5%Pt/ γ-Al_2O_3 (50.8%) > 5% Ru/Al_2O_3 (39.7%), while at catalyst to oil weight ratio of 0.088, following trend was obtained: 66%Ni/SiO_2-Al_2O_3 (95.9%) > sulfided NiMo/γ-Al_2O_3 (91.9%) > 5% Pd/γ-Al_2O_3 (90.9%) > sulfided CoMo/γ-Al_2O_3 (80%). Hydrocarbons in the diesel range were produced mostly while sulfided CoMo/γ-Al_2O_3 produced considerable amounts of jet fuel and naphtha.

d) Effect of catalyst particle size.

In the SDO of methyl oleate, Ni metal and Ni_2P supported on SBA-15 showed almost 80% conversion at 20 h^{-1} WHSV for the temperatures higher than 290 ºC and pressure equal to 30 bar. But it was found that Ni_2P particles with average diameter of 7 nm were well dispersed within the mesopores of SBA-15 while metallic Ni were larger in size (~25-60 nm) and were spread out on the surface of support.

Chapter 3

Experimental

The materials used in this research were methyl oleate, commercial biodiesel, ammonium meta-tungstate, ammonium tetrathio-tungstate, ammonium hydroxide, nickel nitrate hexahydrate, (heptadecane & octadecane for calibration) and γ-alumina. All of these materials were purchased from Sigma-Aldrich Company, St. Louis, MO and commercial biodiesel was purchased from Diesel-Direct Company, Stoughton, MA.

3.1 WO_3 /γ-Al_2O_3 catalyst preparation

15 g of Ammonium meta-tungstate was dissolved in 50 mL water and 15 mL ammonium hydroxide solution to form a uniform saturated solution. Impregnation was carried out at room temperature by introducing 25 g of γ-alumina to this saturated solution and blanketed under nitrogen gas at room temperature (25ºC) for 24 h. The equilibrated γ-alumina was separated by filtration and then calcined in an oven at 400ºC for 2 h. This calcining procedure thermally decomposed the Ammonium meta-tungstate into immobilized WO_3 on γ-Al_2O_3 according to the equation:

$$(NH_4)_6(H_2W_{12}O_{42})\cdot 4H_2O \rightarrow 12WO_3 + 6NH_3 + 8H_2O + O_2$$

Finally, all prepared WO_3/γ-Al_2O_3 samples were cooled under nitrogen gas and stored at room temperature for future use. The surface area of catalysts was evaluated by the Brunauer-Emmett-Teller method (BET), and the loading of tungsten and promoted tungsten was characterized by X-ray Photoelectron Spectroscopy method (XPS).

3.2 $NiWO_4/\gamma\text{-}Al_2O_3$ catalyst preparation

Nickel is present as $NiWO_4$ and $NiAl_2O_4$ as per study by Ng and Hercules (1976, [8]). They showed that pretreatment of the Nickel promoted catalyst with H_2 reduces Nickel species to Ni metal on the surface whereas WO_3 is quite stable compared to nickel aluminate and nickel tungstate [8].

5 g of Nickel nitrate hexahydrate were dissolved in 40 mL water to form a solution at room temperature (25ºC) and 150 rpm. Then 15 g of $WO_3/\gamma\text{-}Al_2O_3$ were added to this solution and blanketed in air at room temperature for 48 h. Finally, the solid catalyst was collected by filtration and dried in a vacuum desiccator at room temperature for 24 h to get $NiWO_4$ according to the ionic equation,

$$WO_4^{2-} + Ni^{2+} \rightarrow NiWO_4$$

The $NiWO_4/\ \gamma\text{-}Al_2O_3$ catalyst was characterized by BET and XPS and then stored at room temperature for future use.

3.3 $WS_2/\gamma\text{-}Al_2O_3$ catalyst preparation

Alumina is usually used as a support with NiW or CoMo catalysts because of its high surface area, high thermal stability, high physical strength and recoverability. But alumina support strongly interacts with the metal oxide and thus hinders its sulfidation. For instance, the Mo-O bond is weaker than W-O bond thus it is more difficult to transform WO_3 to WS_2 and also require high temperatures and high H_2S/H_2 ratios or high DMDS (Dimethyl Disulfide) therefore we have used sulfided W complex as the precursor to get WS_2 catalyst [29]. The catalyst was prepared by wet impregnation as described in the literature [30 – 34].

15 g of Ammonium tetrathio-tungstate were dissolved in 50 mL of water and 15 mL of ammonium hydroxide to form a uniform saturated solution. Impregnation was carried out at room temperature by introducing 25 g of γ-alumina to this saturated solution and blanketing under nitrogen gas at room temperature (25ºC) for 24 h. The equilibrated catalyst was separated by vacuum filtration and nitrogen gas was blown over it to maintain an inert atmosphere. The separated catalyst was dried under vacuum desiccator for 24 h and then stored under nitrogen for future use. Supported catalyst was thermally decomposed in the reactor with H_2 to give WS_2 according to the equation below.

$$(NH_4)_2WS_4 + yH_2 \rightarrow (NH_4)_2S + yH_2S + WS_{3-y}$$

3.4 $NiWS_4/\gamma\text{-}Al_2O_3$ catalyst preparation

The catalyst prepared as described in the previous section was used to prepare nickel promoted tungsten sulfide catalyst. 5 g of nickel nitrate hexahydrate were dissolved in 40 mL water to form a solution at room temperature (25ºC) and 150 rpm. Then 15 g of ATT/γ-Al_2O_3 was added to this solution and blanketed in nitrogen at room temperature for 48 h. Finally, the solid catalyst was collected by vacuum filtration and nitrogen gas blown over it and dried in a vacuum desiccator at room temperature for 24 h to get grey colored $NiWS_4$ according to the ionic equation.

$$WS_4^{2-} + Ni^{2+} \rightarrow NiWS_4$$

3.5 Surface area and loading measurements

All the catalysts prepared were evaluated by BET to determine the surface area and by XPS to determine the loading of tungsten and nickel. The details of BET and XPS methods are introduced next, and the results are shown in Tables 2 and 3.

3.6 BET area measurement

The surface area was determined by N_2 adsorption at -195ºC using a Quantasorb analyzer. Nitrogen partial pressure was changed by regulating the flow rate of N_2 in a N_2/He mixture. The incremental volumes adsorbed were detected by a thermal conductivity detector. The corresponding calibration constant was used to convert peak area to adsorbed N_2 volume.

Catalyst	**BET Area (m^2/g)**
$WO_3/\gamma\text{-}Al_2O_3$	191
$NiWO_4/\gamma\text{-}Al_2O_3$	176
$WS_2/\gamma\text{-}Al_2O_3$	100
$NiWS_4/\gamma\text{-}Al_2O_3$	106

Table2. BET Area measurements.

3.7 XPS loading measurement

XPS is a surface-sensitive quantitative spectroscopic technique that measures the elemental composition at the parts per thousand range, empirical formula, chemical state and electronic state of the elements that exist within a material. XPS spectra were obtained by irradiating the sample with a beam of X-rays while simultaneously measuring the kinetic

energy and number of electrons that escape from the top 0 to 10 nm of the material being analyzed. Usually XPS requires high vacuum (P ~10^{-8} millibar) or ultra-high vacuum (P < 10^{-9} millibar) conditions. The loadings of catalysts were calculated with the data for mass of W and Ni, as well as the total mass tested.

Catalyst	W wt%	Ni wt%
$WO_3/\gamma\text{-}Al_2O_3$	6.99%	-
$NiWO_4/\gamma\text{-}Al_2O_3$	4.91%	1.46%
$WS_2/\gamma\text{-}Al_2O_3$	14.07%	-
$NiWS_4/\gamma\text{-}Al_2O_3$	24.47%	5.05%

Table 3. XPS Catalyst loading measurements.

3.8 Equipment setup and reaction procedure

3.8.1 Reaction setup

Typically, the catalytic HDO process contains three steps: (i), pretreatment of the catalyst by hydrogen gas to reduce WO_3 and/or NiO; (ii), reaction step with biodiesel and hydrogen gas, with samples periodically analyzed by gas chromatography (GC); and (iii), cleaning and drying step of catalyst by inert gas. Based on these steps, an auto-sampling bubbler-reactor system was designed and assembled, as shown in Fig. 3.1.

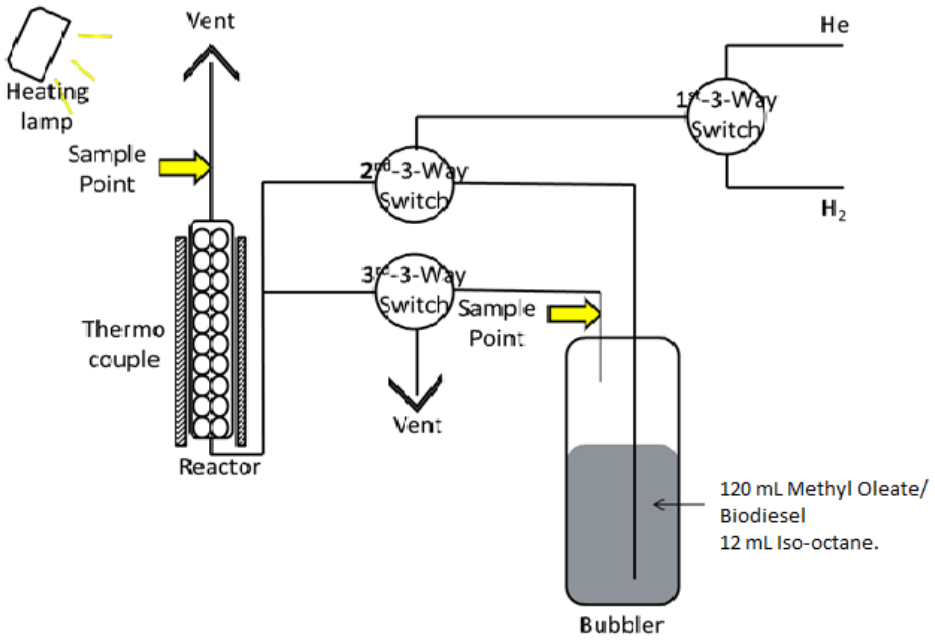

Fig. 3.1 Reaction system setup.

The system essentially consisted of a stainless-steel micro-reactor (1/4×17/4 in.) and a stainless-steel bubbler (5/4×17/4in.) equipped with three 3-way valves that permitted *in situ* pretreatment, reaction, and activity measurement of the catalyst. The lines between the bubbler, the microreactor, and the line downstream of the reactor were stainless-steel coil (1/4 in.) wrapped with heating tape to prevent condensation of reactants. There also were heating lamps around the whole system to provide a constant temperature environment. All the sample points were covered with silica septa and the samples were taken by a gas-proof pressure-lock syringe and analyzed by gas chromatography (Hewlett Packard 5890). The reactor was loaded with 0.1 g of catalyst as well as glass wool, and the bubbler was loaded

with 120 mL biodiesel or methyl oleate and 12 mL iso-octane. The detail of valves set in every reaction step will be described in the next section.

3.8.2 Pretreatment step

In this step, the first 3-way valve was set to connect the hydrogen gas to the system, and the second valve was set to connect the inlet gas directly to the reactor. The third valve was set to connect the bubbler to the vent, as shown in Fig. 3.2. 60 mL/min of the hydrogen gas flowed through the microreactor to reduce the catalyst. The temperature of reactor was set at 250ºC, 300ºC, 350ºC or 400ºC and the reduction was carried out for 1 h. Previous literature works [31, 32] have shown that reduction carried for 1 h or more has no effect on the catalyst functioning. If the catalyst is unreduced then it will not have any activity.

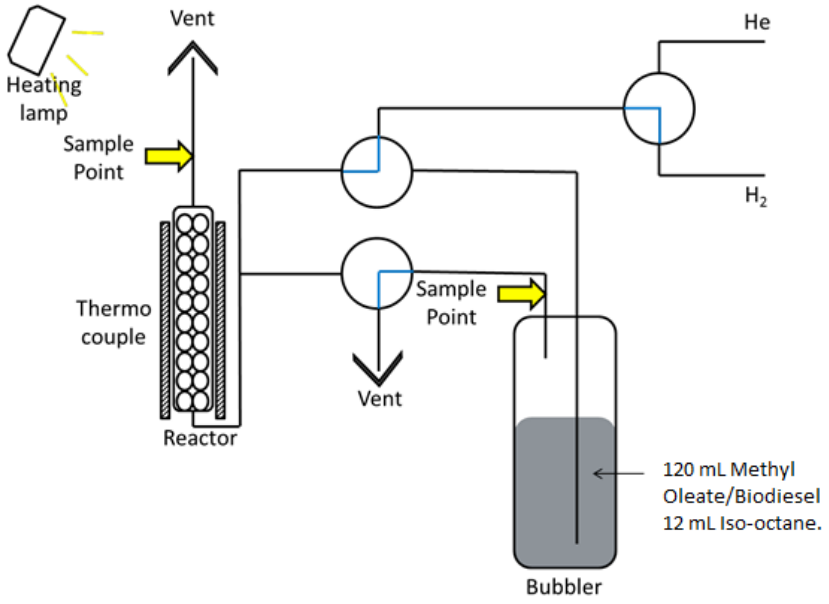

Fig. 3.2 Valves set-up for pretreatment step.

3.8.3 Reaction step and sample analysis

In this step, the first 3-way valve was set to connect the hydrogen gas to the system, the second valve was set to connect the inlet gas to the bubbler, and the third valve was set to connect the outlet of bubbler to the reactor, as shown in Fig. 3.3. The reactor temperature was set at 350ºC or 400ºC and the hydrogen flow rate was set at 60 mL/min. 0.3 mL of gas sample of the final product was taken by a gas-proof pressure-lock syringe at a reaction time of 60 min. Inlet samples (at the outlet of bubbler) of 0.3 mL was taken before the reaction step. All samples were analyzed by gas chromatography (Hewlett Packard 5890, detector: FID). In the analysis step, helium gas was used as a carrier for the GC and the flow rate was set at 2.52 mL/min. Hydrogen and compressed air were used for the FID, and the flow rates were set at 30.8 mL/min and 300 mL/min, respectively. The injector temperature of GC was kept at 180ºC and the detector temperature at 350ºC. The initial temperature of the GC oven was set at 180ºC, and this temperature was kept for 2 min. Then the oven temperature was increased to 220ºC at a rate of 10ºC/min. The final temperature of 220ºC was kept for 30 min. The data were transferred to a computer with the help of Peak96. The data files were analyzed by software Origin-8 to calculate the areas of all peaks. With the help of a calibration line shown in Appendix B, the concentration of initial biodiesel, final biodiesel, C_{18} green diesel, and C_{17} green diesel were calculated from the area results. Finally, the total conversion of biodiesel, green diesel's C_{18}/C_{17} ratio (for the pathway selectivity) were calculated from these data, as shown in Appendix C.

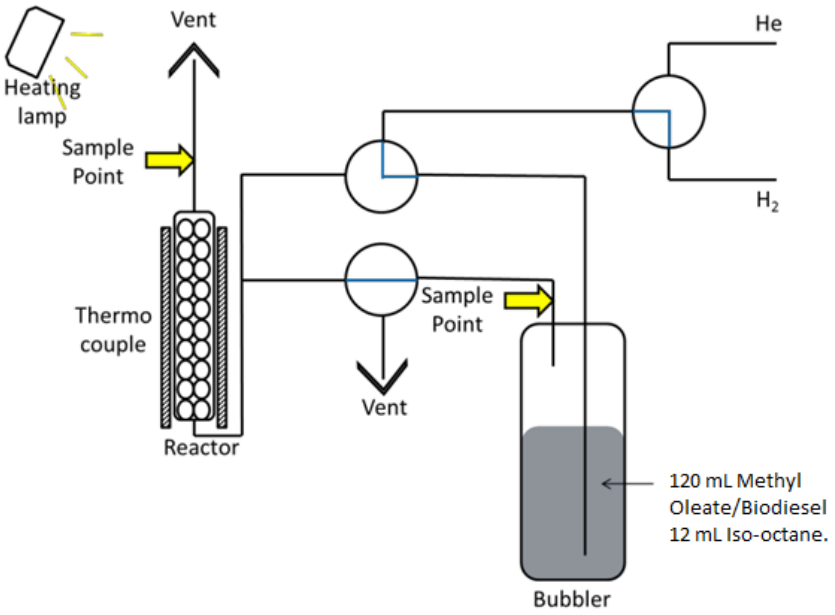

Fig. 3.3 Valves set-up for reaction step.

3.8.4 Post-reaction cleanup step

In this step, the first 3-way valve was set to connect the helium gas to the system, the second valve was set to connect the inlet gas directly to the reactor, and the third valve was set to connect the bubbler to the vent, as shown in Fig. 3.4. 20 mL/min of helium gas was used to blow out all reactant residues as well as water produced in the reaction. The temperature of reactor was kept at 200ºC and this step lasted for 1 h.

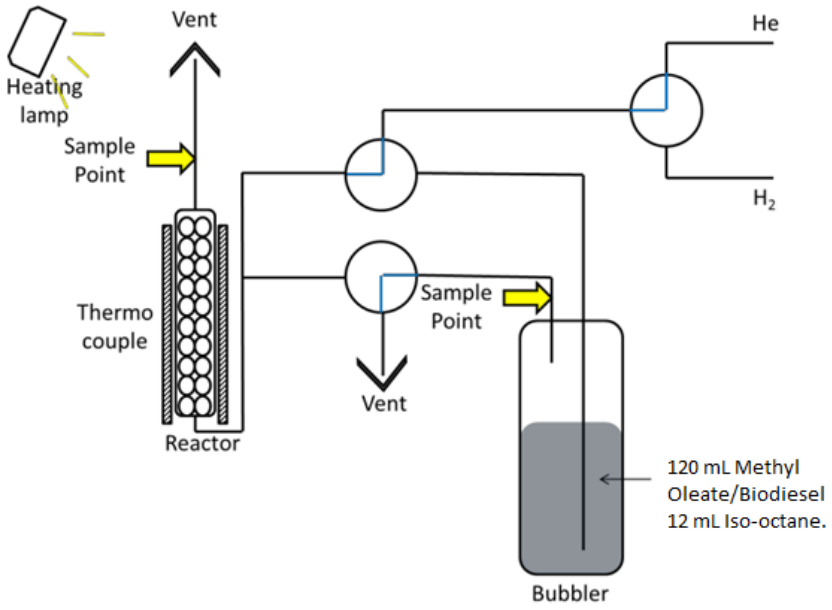

Fig. 3.4 Valves set-up for post-reaction cleanup step.

3.9 Catalyst activity investigation

3.9.1 Effect of feedstock

In this research, two sources of biodiesel (ACS grade methyl oleate, which served as a model compound, from Sigma - Aldrich and commercial biodiesel B100 from Diesel Direct) were investigated. 120 mL of biodiesel (methyl oleate or commercial biodiesel B100) and 12 mL of isooctane were loaded into the bubbler, and 0.1 g of catalyst was loaded into the reactor. The pretreatment temperature was set at 250ºC, 300ºC, 350ºC or 400ºC and the pretreatment hydrogen flow rate was set at 60 mL/min. The reaction temperature was set at 350ºC or 400ºC and hydrogen flow rate during the reaction step was also set at 60 mL/min.

The final product samples were taken at 1, 2, 3 and 4h respectively. Reaction inlet sample was taken before the reaction step. All samples were tested by GC and the conversions were calculated.

3.9.2 Effect of pretreatment temperature and/or reaction temperature

In this experiment, 120 mL of Biodiesel and 12 mL of isooctane were loaded into the bubbler, and 0.1g of hydrodeoxygenation catalyst (WO_3/γ-Al_2O_3) was loaded into the reactor. Four pretreatment temperatures (250ºC, 300ºC, 350ºC or 400ºC) were investigated. The pretreatment hydrogen flow rate was set at 60 mL/min, the reaction temperature set at 350ºC or 400ºC, and hydrogen flow rate during the reaction step was also set at 60 mL/min. The final product samples were taken at 1, 2, 3 and 4 h respectively. Reaction inlet sample was taken before the reaction step. Samples were tested by GC and the conversion was calculated. Conversions of different pretreatment temperatures were then compared.

3.9.3 Effect of hydrogen flow rates

In this experiment, 120 mL of Biodiesel and 12 mL of isooctane were loaded into the bubbler, and 0.1g of hydrodeoxygenation catalyst (WO_3/γ-Al_2O_3) was loaded into the reactor. Three hydrogen flow rates (40, 60 and 80 mL/min) during the reaction step were investigated at reduction temperature of 300ºC and reaction temperature of 400ºC. The rest of the procedure was similar to the one described in the previous section.

3.9.4 Effect of promoter

In this experiment, 120 mL of Biodiesel and 12 mL of isooctane were loaded into the bubbler, and 0.1g of hydrodeoxygenation catalyst (Ni-W/γ-Al_2O_3) was loaded into the reactor. The pretreatment temperature was set at 300ºC, the pretreatment hydrogen flow rate set at 60 mL/min, the reaction temperature set at 400ºC and the hydrogen flow rate during the reaction step was set at 60 mL/min. The final product samples were taken at 1, 2, 3 and 4 h respectively. Reaction inlet sample was taken before the reaction step. Samples were tested by GC and the conversion was calculated. Conversions and yields were then compared with unpromoted catalyst.

3.9.5 Comparison between oxide and sulfide catalyst

In this experiment, 120 mL of Biodiesel and 12 mL of isooctane were loaded into the bubbler, and 0.1g of hydrodeoxygenation catalyst (WS_2/γ-Al_2O_3) was loaded into the reactor. The pretreatment temperature was set at 300ºC, the pretreatment hydrogen flow rate set at 60 mL/min, the reaction temperature set at 400ºC and the hydrogen flow rate during the reaction step was set at 60 mL/min. The final product samples were taken at 1, 2, 3 and 4 h respectively. Reaction inlet sample was taken before the reaction step. Samples were tested by GC and the conversion was calculated. Conversion of methyl oleate using unpromoted and promoted sulfide catalyst were then compared with oxide catalyst.

3.9.6 Effect of continuous usage of catalyst

In this experiment, 120 mL of Biodiesel and 12 mL of isooctane were loaded into the bubbler, and 0.1g of hydrodeoxygenation catalyst ($WO_3/\gamma\text{-}Al_2O_3$) was loaded into the reactor. The pretreatment temperature was set at 300ºC, the pretreatment hydrogen flow rate set at 60 mL/min, the reaction temperature set at 400ºC and the hydrogen flow rate during the reaction step was set at 60 mL/min. The catalyst was used again on the second day and the activity of the catalyst was compared with unused/reduced catalyst. The rest of the procedure was identical.

CHAPTER 4

Results and Discussion

4.1 Effect of feedstock

Commercial biodiesel is a complex mixture of fatty acid methyl esters. It has 49–57 vol% of the component methyl oleate ($C_{17}H_{33}O_2CH_3$), 18–30 vol% methyl linoleate ($C_{17}H_{31}O_2CH_3$), 8–13 vol% methyl palmitate ($C_{15}H_{31}O_2CH_3$), as well as small amounts of methyl stearate ($C_{17}H_{35}O_2CH_3$) and methyl linolenate ($C_{17}H_{29}O_2CH_3$). Evaluation of commercial biodiesel is usually a complex task, and ACS grade methyl oleate is typically used as a model compound for biodiesel.

In this research, ACS grade methyl oleate and commercial biodiesel B100 were used to run the hydrodeoxygenation process using tungsten catalyst promoted with Ni. The results of overall methyl oleate and biodiesel conversions are shown in Fig. 4.1.

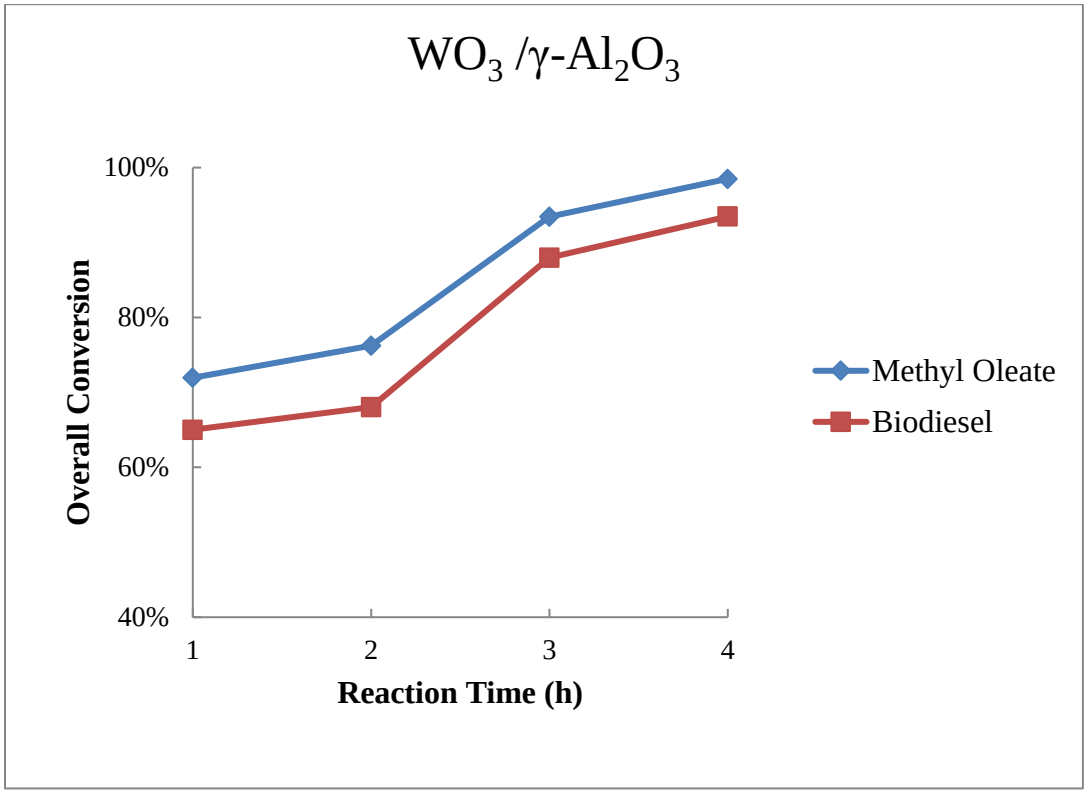

Fig. 4.1 Overall methyl oleate/biodiesel conversions. Catalysts loadings were 0.1±0.05 g.

Operating conditions: Reduction temperature: 300 ºC

Reaction temperature: 400 ºC

Hydrogen flowrate: 60 mL/min

From this result, we can find that the overall conversions of methyl oleate and commercial biodiesel are almost the same, with methyl oleate a little higher than commercial biodiesel (98.5% versus 93.5%). As commercial biodiesel contains some amount of saturated

fatty acid esters, its reactivity is a little less than ACS grade methyl oleate which is 70% methyl oleate and 30% methyl linoleate (by weight) both of which are unsaturated fatty acid esters. Additionally, the C_{18}/C_{17} ratios of the final product are found to be 6.5 versus 5.7. This result proves that the reactivity is less with commercial biodiesel as compared to methyl oleate.

4.2 Effect of pretreatment temperature

Pretreatment is an important step to promote and maintain the activity of the catalyst. In the catalytic HDO process, pretreatment of the catalyst by hydrogen at a certain temperature reduces the metal oxide and provides the active sites used in further reaction steps. This reduction procedure is mainly affected by temperature thus study of the pretreatment temperature is an important and necessary step.

In this research, four pretreatment temperatures were tested, namely, 250°C, 300°C, 350°C and 400°C. It is found that conversion of methyl oleate/biodiesel increases with increase in reduction temperature, but the yield of green diesel and ratio of C_{18}/C_{17} is optimal at a reduction temperature of 300°C as shown in Fig. 4.2 and Fig. 4.3.

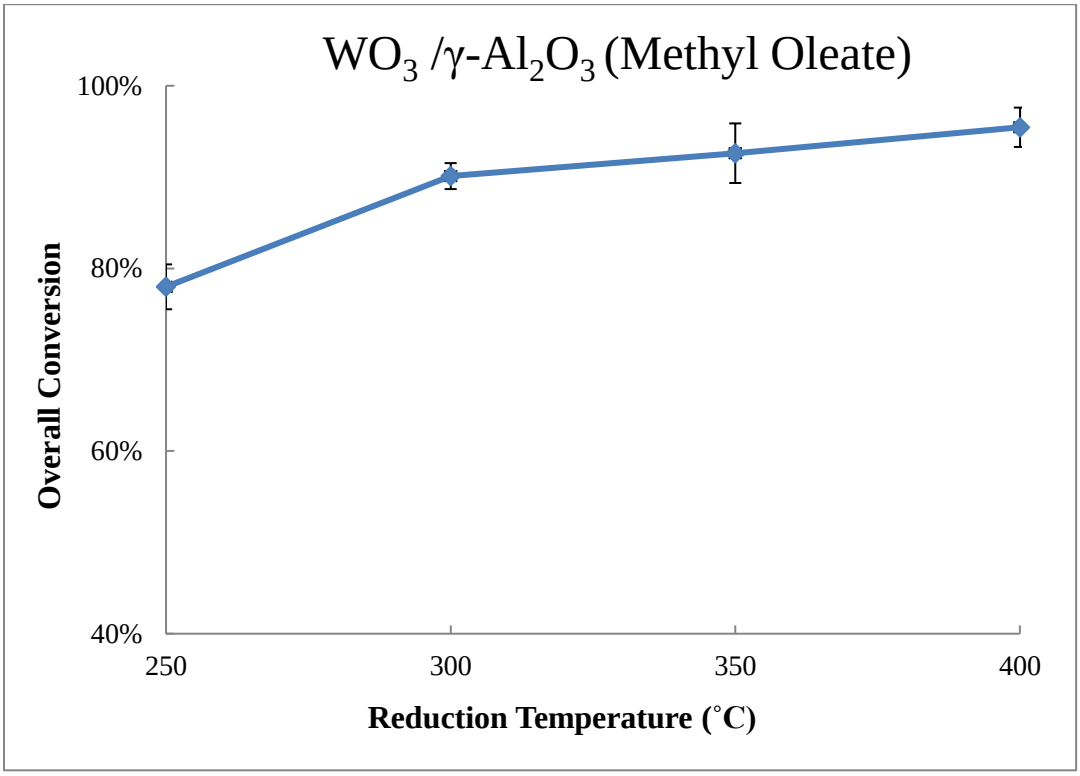

Fig. 4.2 Effect of reduction temperature on overall conversion.

Operating conditions: Reaction temperature: 400 ºC

Hydrogen flowrate: 60 mL/min

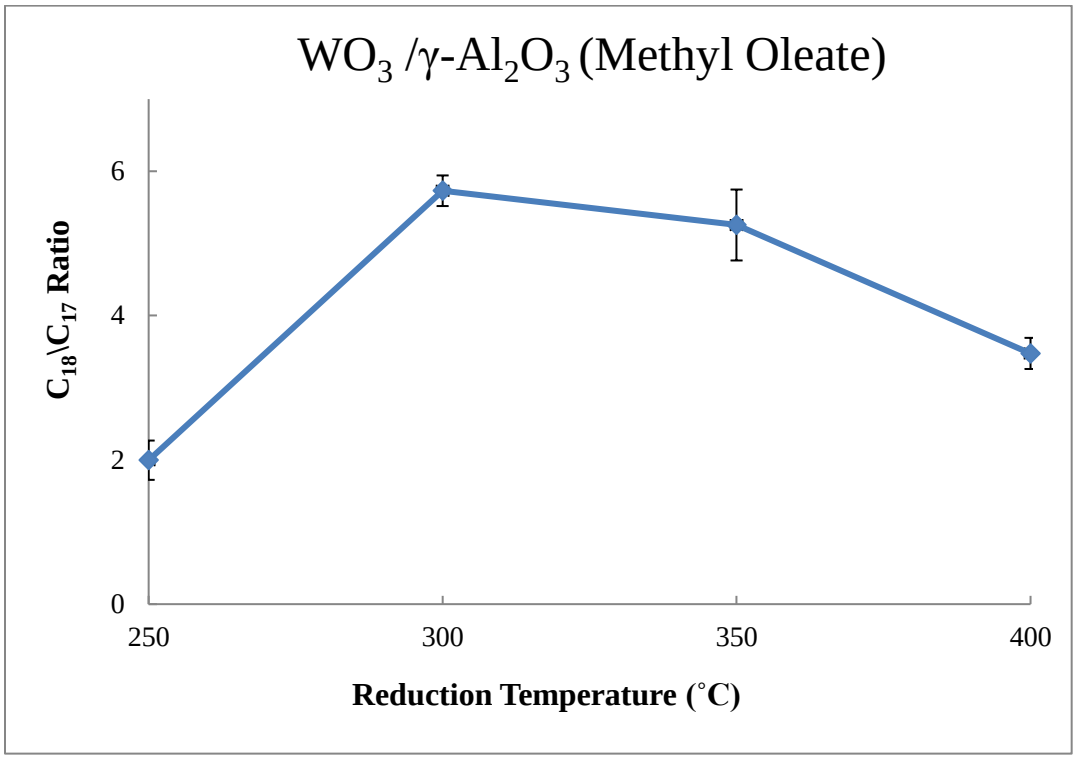

Fig. 4.3 Effect of reduction temperature on C_{18}/C_{17} ratio.

Operating conditions: Reaction temperature: 400 ºC

Hydrogen flowrate: 60 mL/min

Moreover, with $WO_3/\gamma\text{-}Al_2O_3$ catalyst, at lower reduction temperatures of 250°C, conversion is 82% and selectivity towards kerosene and gasoline range products (than green diesel) is ~85%. Oxidic support of the metal catalyst also facilitates hydrocracking and shifts the product distribution to gasoline-range products apart from hydrogenation [7]. It is anticipated that WO_3 catalyst interacts with the $\gamma\text{-}Al_2O_3$ support to form $Al_2(WO_4)_3$ [8], which leads to the cracking of hydrocarbon chain of the fatty acid methyl ester as per following reaction mechanism.

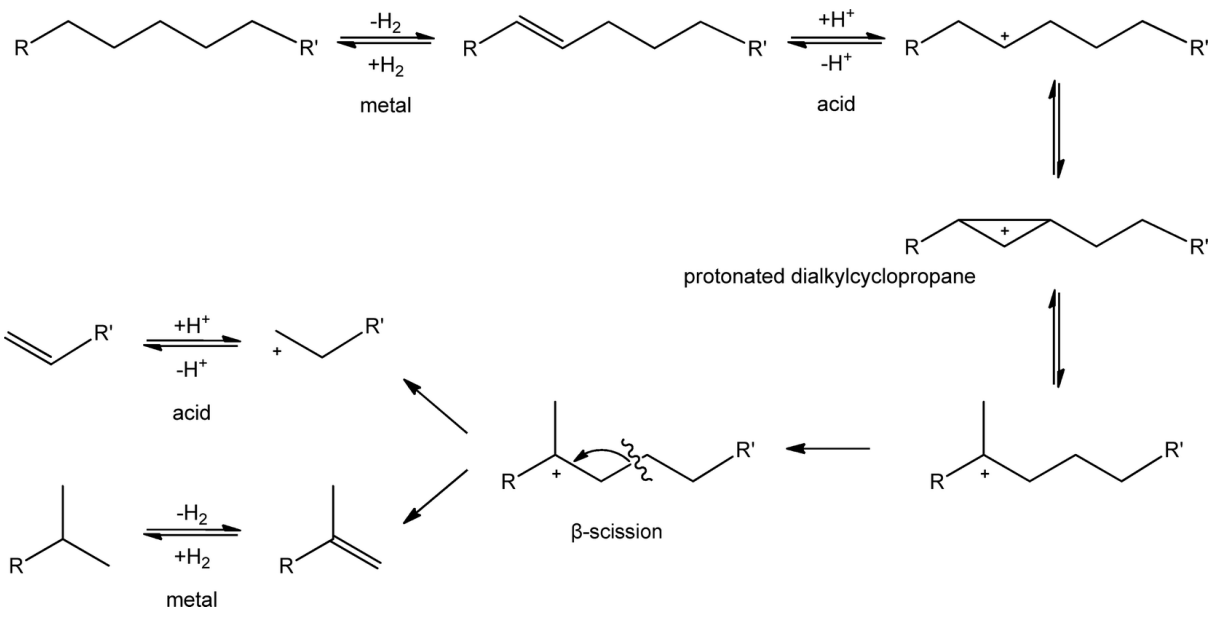

Fig. 4.4 Hydrocracking reaction mechanism.

The double bond of fatty acid chain is first hydrogenated and then cracking reaction takes place. Aluminium Tungstate being a Lewis acid, donates H^+, and this proton attacks the double bond of the hydrocarbon chain to crack the molecules as shown in Fig. 4.4.

4.3 Effect of hydrogen flowrate

Hydrogen pressure plays a key role in the hydrodeoxygenation process, especially in overall biodiesel conversion and deoxygenation pathway selection. Additionally, hydrogen gas also acts as a carrier gas for biodiesel in the experimental system, so the mass of biodiesel in the system is affected by hydrogen flow rate. In this study, three hydrogen flow rates (40, 60 and 80 mL/min) were investigated with the $WO_3/\gamma\text{-}Al_2O_3$ catalyst. The result of mass of biodiesel input in 3 mL inlet gas sample is shown in Fig. 4.5.

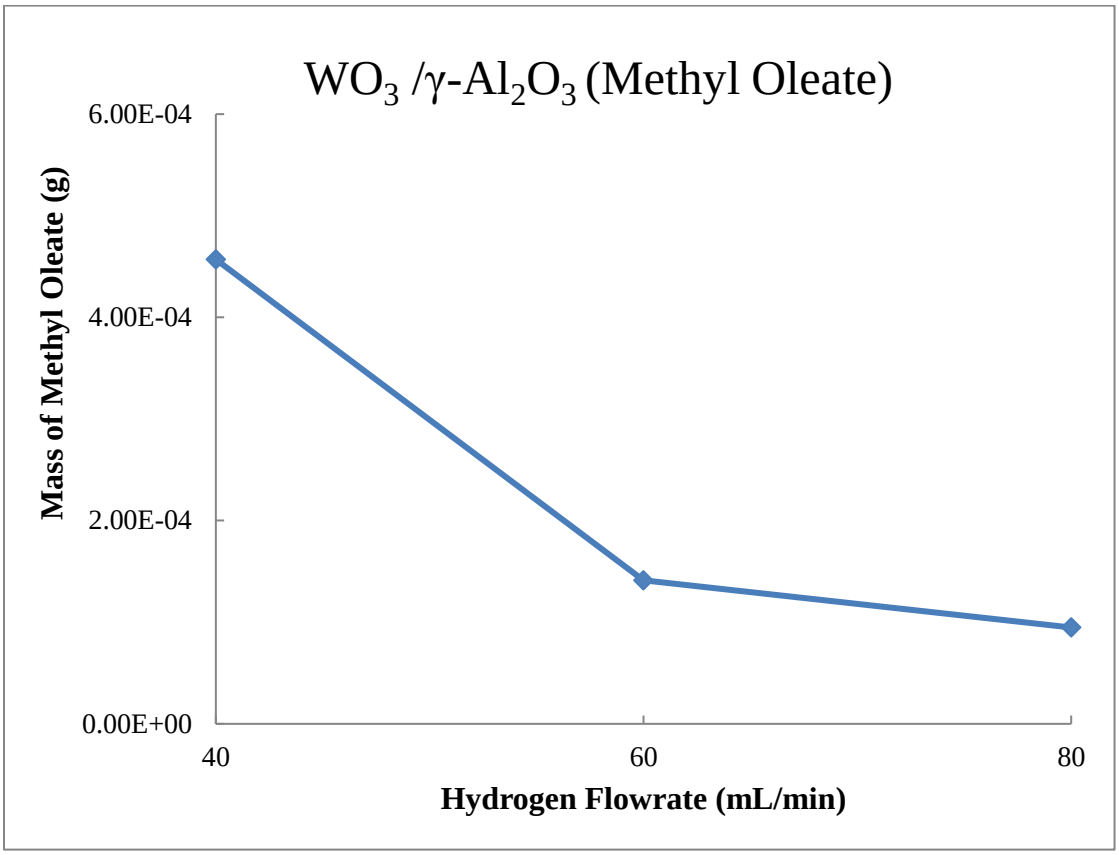

Fig. 4.5 Mass of Methyl Oleate input at different hydrogen flow rate.

Operating conditions: Reduction temperature: 300 ºC

Reaction temperature: 400 ºC

From this data, the Linear Hourly Space Velocity can be calculated. The LHSV of methyl oleate decreased from 6.30 h^{-1} to 0.76 h^{-1} when hydrogen flow rate was increased from 40 mL/min to 80 mL/min, as shown in Fig. 4.6. External mass transport can be enhanced by a better mixing of the fluid. A higher flowrate of hydrogen contributes to enhanced mass transfer by reducing the laminar film around the catalyst particle and ensuring that more reactants are transported to the surface of the catalyst. At low flowrates of hydrogen, it is also conceivable

that there is more adsorption of methyl oleate or biodiesel on the catalyst leading to reduction in surface area. Consequently, the overall conversion of the reactants can be increased in spite of lowering the residence time.

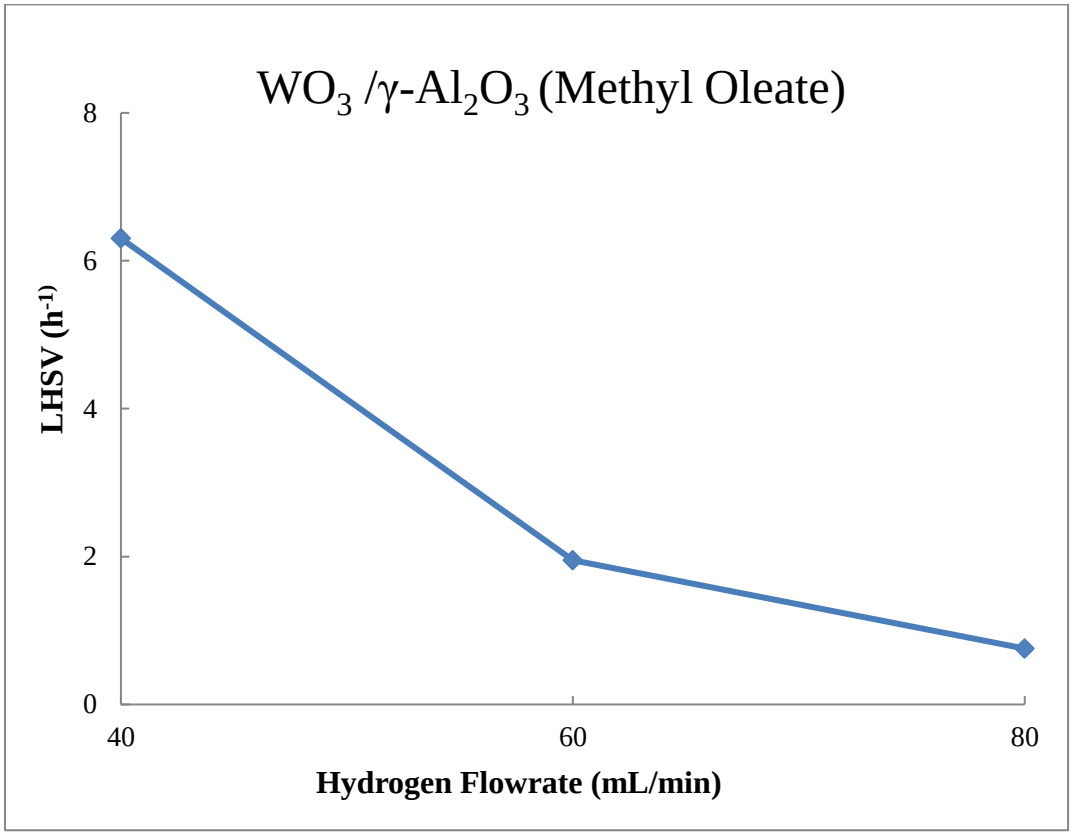

Fig. 4.6 LHSV of methyl oleate input with different hydrogen flow rate.

Operating conditions: Reduction temperature: 300 ºC

Reaction temperature: 400 ºC

Also, the overall methyl oleate conversion and product C_{18}/C_{17} ratio with different hydrogen flow rates were determined and are shown in Fig. 4.7 and Fig. 4.8.

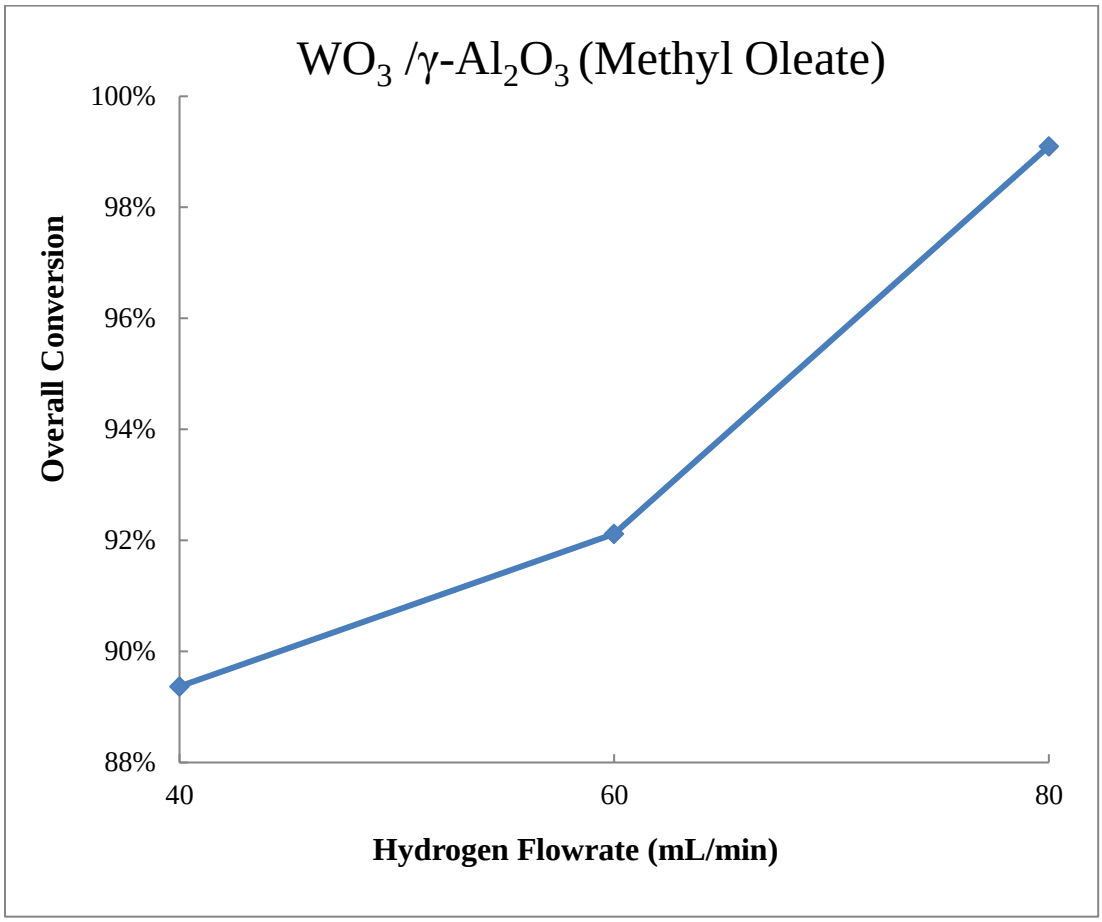

Fig. 4.7 Effect of hydrogen flowrates on overall conversion.

Operating conditions: Reduction temperature: 300 ºC

Reaction temperature: 400 ºC

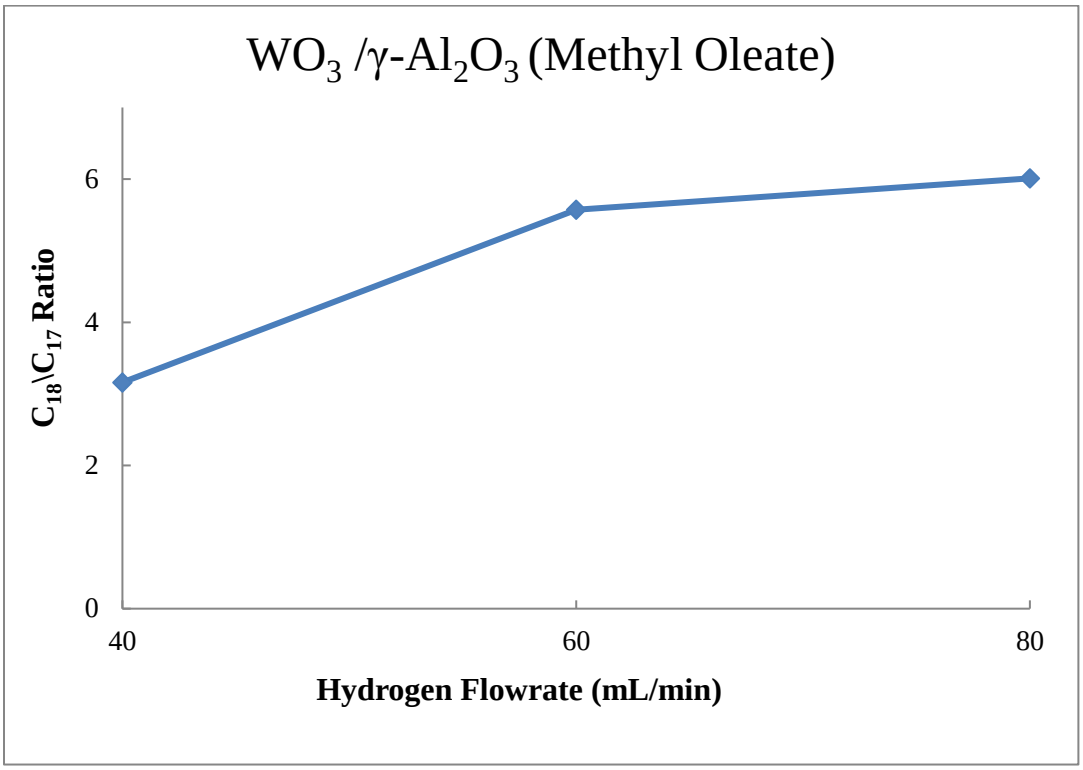

Fig. 4.8 Effect of hydrogen flowrates on C_{18}/C_{17} ratio.

Operating conditions: Reduction temperature: 300 ºC

Reaction temperature: 400 ºC

It is clearly found from Fig. 4.5 and Fig. 4.6 that as hydrogen gas flow rate increases, the mass of methyl oleate per unit volume of gas decreases, which also means an increase in hydrogen partial pressure. Fig. 4.7 shows that this increased hydrogen pressure can benefit the overall conversion, which increased from 89.4% to 99.1% as the H_2 flow rate increased from 40 mL/min to 80 mL/min. There are probably two reasons: (1) because hydrogen is also a carrier gas, higher hydrogen flow rate can produce a higher bulk flow rate that benefits the mass-transfer rate, and (2) the mass of methyl oleate per volume of input gas decreases, which

results in a higher hydrogen/methyl oleate ratio and a higher partial pressure of H_2. This benefits the hydrodeoxygenation reaction.

A higher product C_{18}/C_{17} ratio means that the hydrodeoxygenation pathway also benefits from the higher hydrogen pressure as shown in Fig. 4.8. The stoichiometry of the reactions indicates that more hydrogen is required in the hydrodeoxygenation pathway than the decarbonylation/decarboxylation pathway. Moreover, from the mechanism of the HDO process, it is clear that more gaseous products are formed in the decarbonylation and decarboxylation pathways, which mean they are more favorable at lower reaction pressures. Thus, higher hydrogen pressure will shift the reaction towards the HDO pathway at the expense of other two pathways. Considering all these benefits, a hydrogen flow rate of 60 mL/min provided the optimal condition and was applied in other experimental runs.

4.4 Effect of reaction temperature

Reaction temperature is the most important factor that affects the HDO process and catalyst selectivity. In this study, three reaction temperatures (250ºC, 350ºC and 400ºC) were investigated in the HDO process. From Fig. 4.9 it is clear that a reaction temperature of 400 ºC is optimum. The main reason is that increase of reaction temperature benefits the reaction rate and equilibrium conversion. Calculation from the stoichiometry of the reaction indicates that the reaction enthalpies (ΔH) of hydrodeoxygenation, decarboxylation, and decarbonylation pathways are 82.5, 31.1, and 72.3 kJ/mol, respectively. Moreover, with increase in temperature, there are more anion vacancies existing in the metal-support component that benefit the reactions [1]. As temperature is increased further, coke formation occurs, which can cover the catalyst's active sites to inhibit the mass-transfer rate and reaction rate.

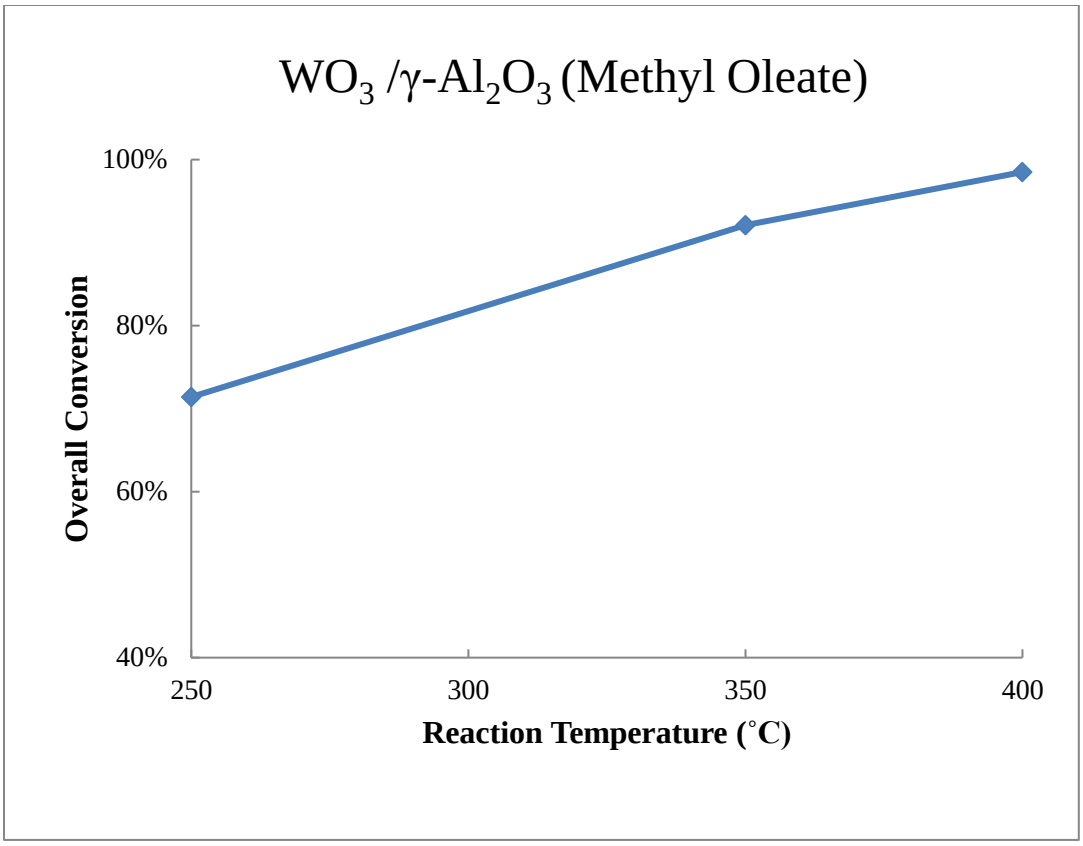

Fig. 4.9 Effect of reaction temperature on overall conversion.

Operating conditions: Reduction temperature: 300 ºC

Hydrogen flowrate: 60 mL/min

4.5 Effect of Promoter

From the results of the experiments, it is found that Ni increases conversion, yield and selectivity of green diesel when used with WO_3 catalyst. It is generally accepted that there are at least two different active sites for the hydrotreating reactions, the edges being occupied by the promoter atoms. Moreover, sulfur anion vacancies associated with the promoter have been found to be more active than those with W atom [5]. The results are shown in figures 4.10 – 4.13.

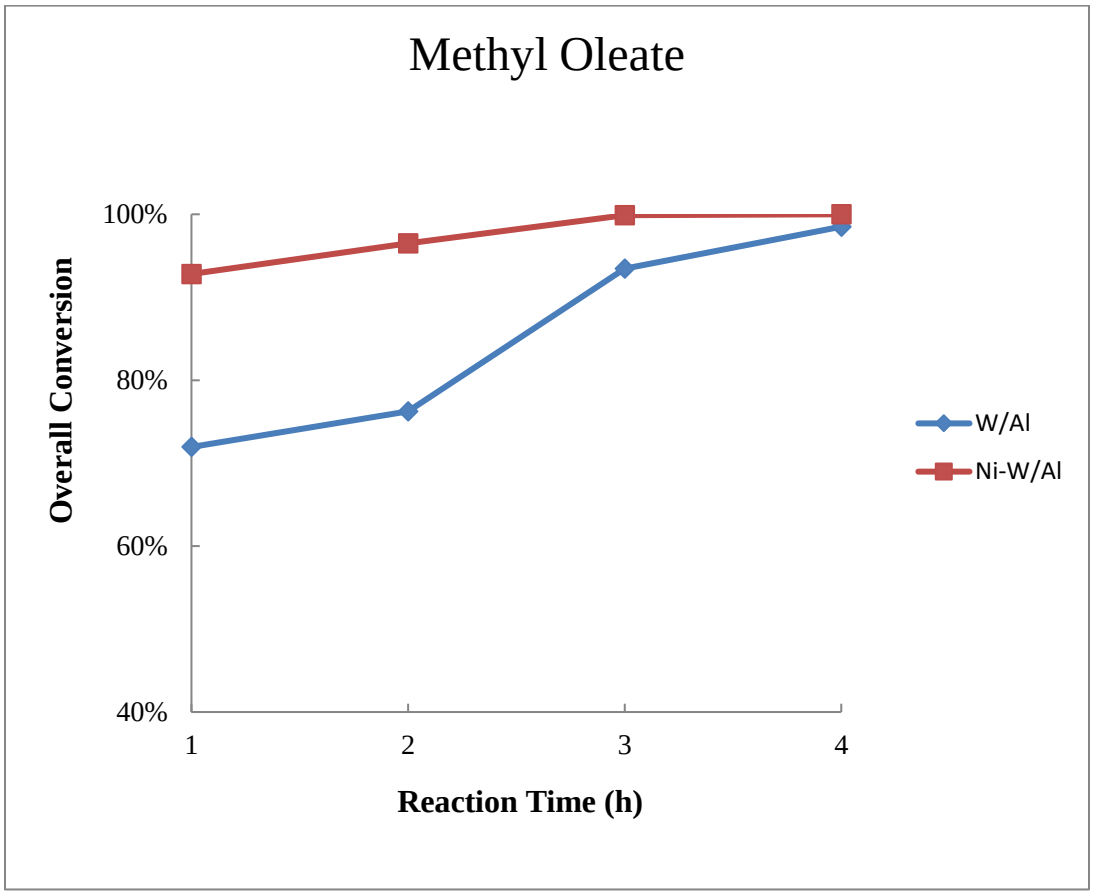

Fig. 4.10 Effect of addition of Ni promoter to W and its comparison on overall conversion when using Methyl Oleate.

Operating conditions: Reduction temperature: 300 ºC

Reaction temperature: 400 ºC

Hydrogen flowrate: 60 mL/min

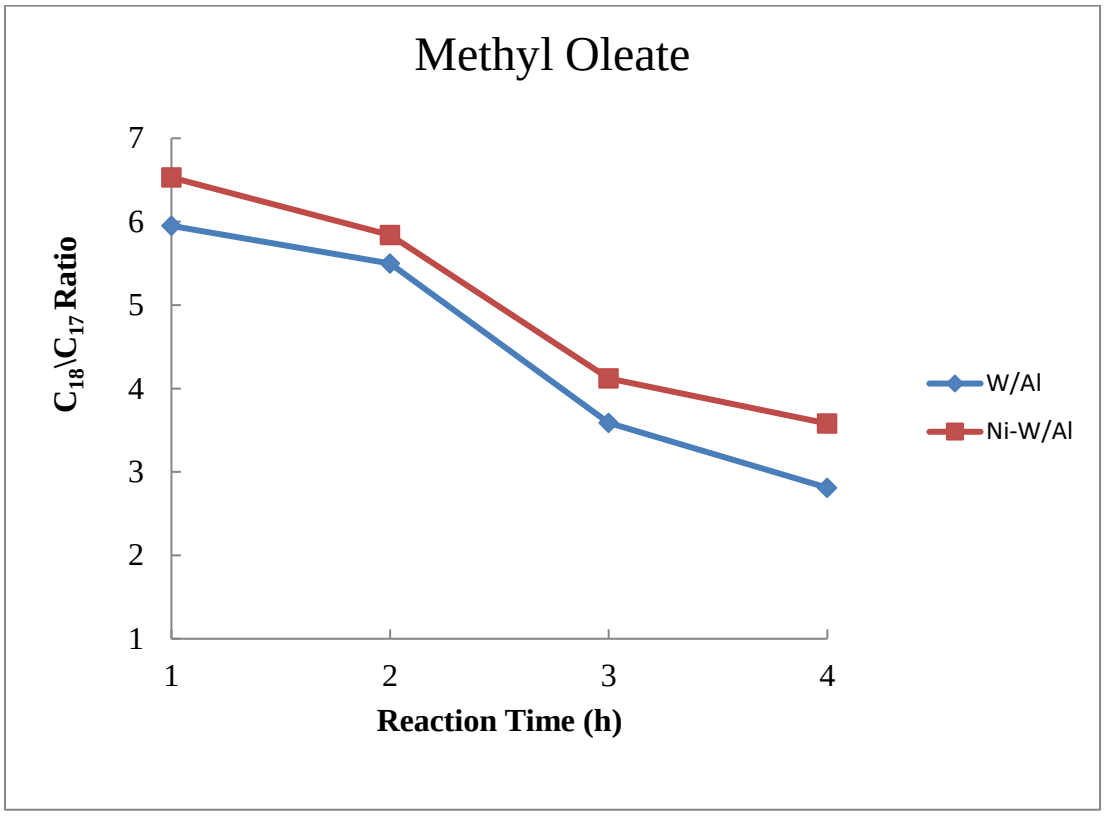

Fig. 4.11 Effect of addition of Ni promoter to W on C_{18}/C_{17} ratio and its comparison when using methyl oleate.

Operating conditions: Reduction temperature: 300 ºC

Reaction temperature: 400 ºC

Hydrogen flowrate: 60 mL/min

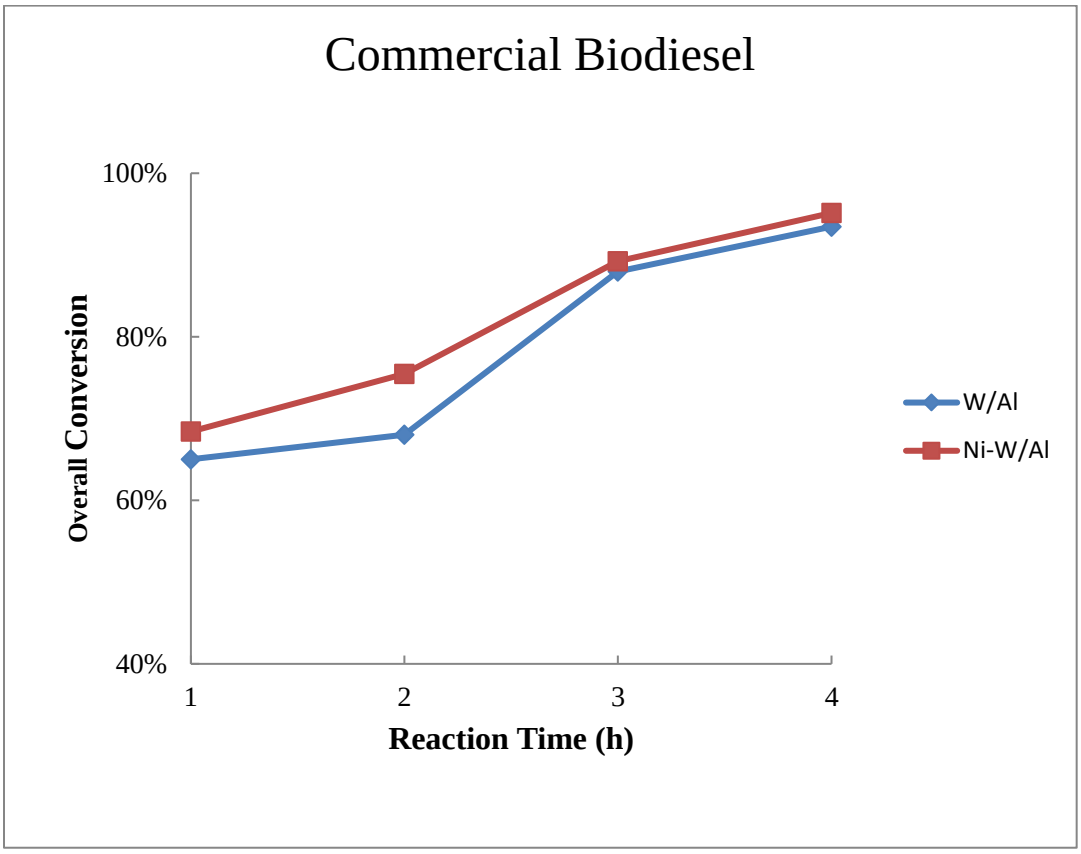

Fig. 4.12 Effect of addition of Ni promoter to W and its comparison on overall conversion when using Commercial Biodiesel.

Operating conditions: Reduction temperature: 300 ºC

Reaction temperature: 400 ºC

Hydrogen flowrate: 60 mL/min

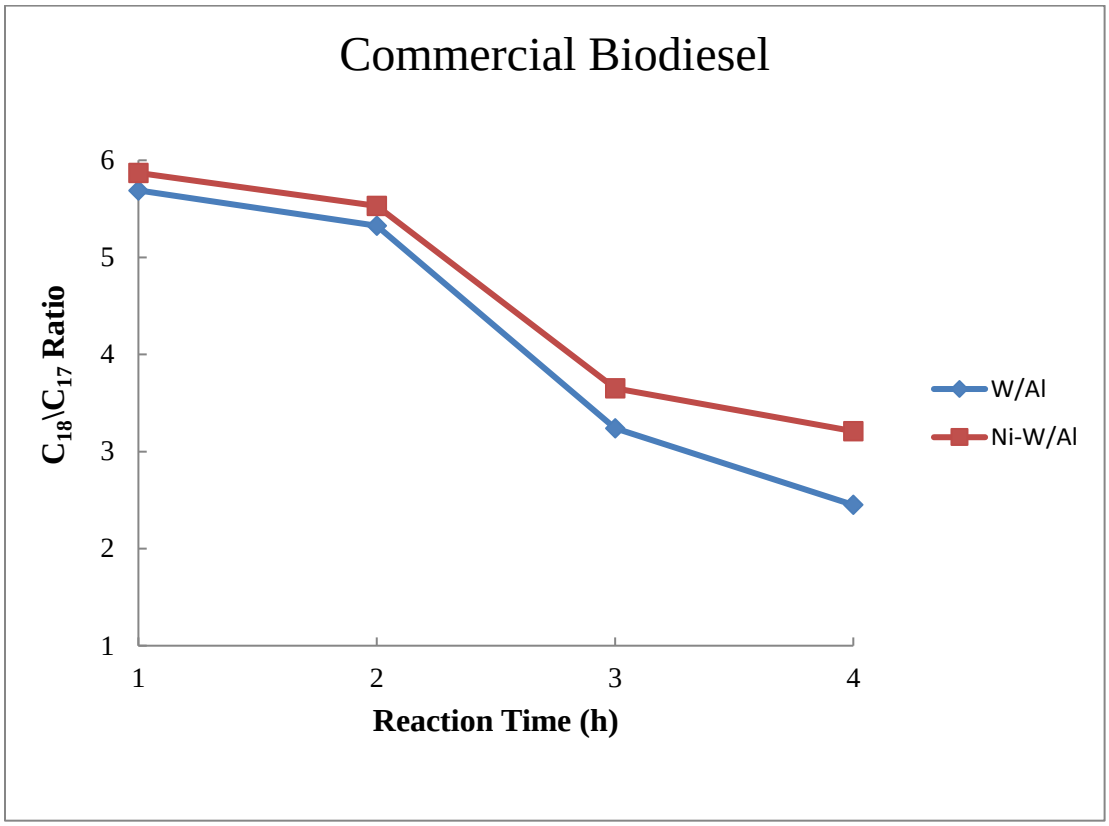

Fig. 4.13 Effect of addition of Ni promoter to W on C_{18}/C_{17} ratio and its comparison when using Commercial Biodiesel.

Operating conditions: Reduction temperature: 300 ºC

Reaction temperature: 400 ºC

Hydrogen flowrate: 60 mL/min

4.6 Comparison between oxide and sulfide catalyst

It is found the introducing anion to the catalyst increases its efficiency in terms of activity, selectivity and overall conversion. It also prevents the catalyst from poisoning. In this research, W catalyst was used in two forms viz, oxide and sulfide. The results of W oxide and sulfide promoted with Ni are shown in the Fig. 4.14. The results from BET analysis show that surface area of oxide catalyst is more than sulfide catalyst. This is due to high metal content in sulfide catalyst than oxide catalyst. Thus, conversion obtained from oxide catalyst is more than sulfide catalyst.

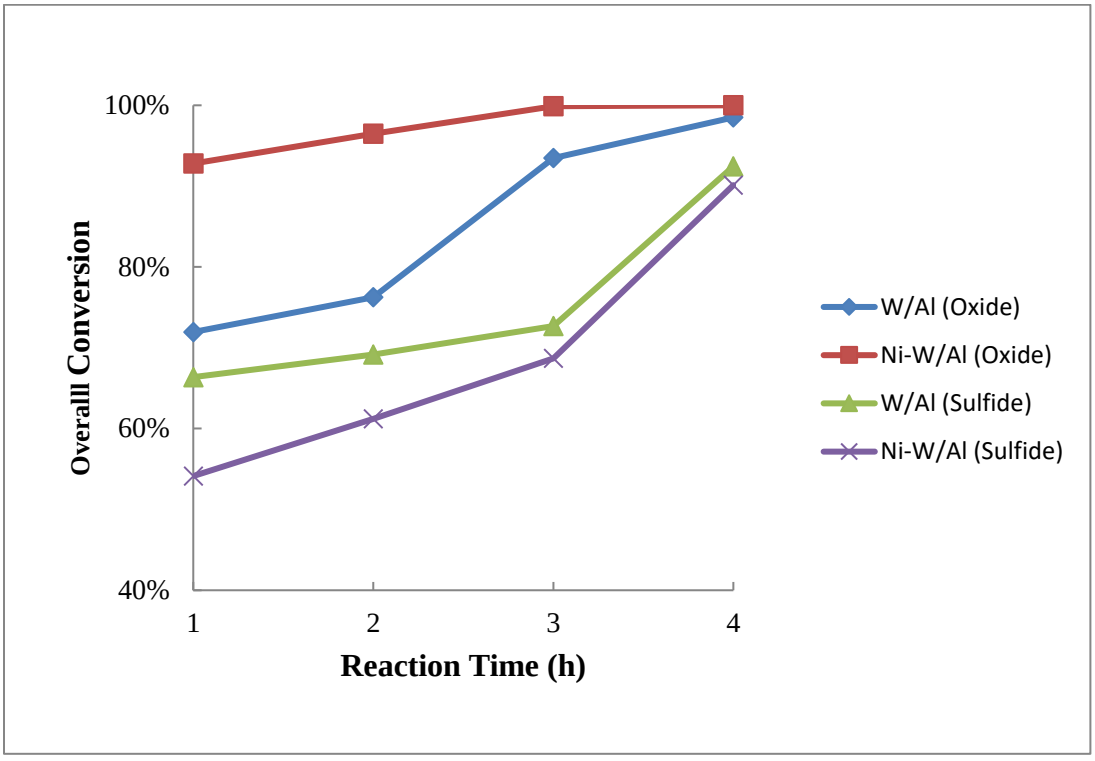

Fig. 4.14 Comparison between oxide and sulfide catalyst.

Operating conditions: Reduction temperature: 300 ºC

Reaction temperature: 400 ºC and Hydrogen flowrate: 60 mL/min

4.7 Effect of continuous usage of catalyst

In this run, the catalyst was reused on the second day with same reduction and reaction time and the results are shown in the Fig. 4.15. It is found that the catalyst gets deactivated with time and there is negligible formation of green diesel and conversion also decreases. A plausible reason for this could be cooling of the reactor and the catalyst followed by heating thus resulting in some deactivation of the catalyst due to loss of surface area.

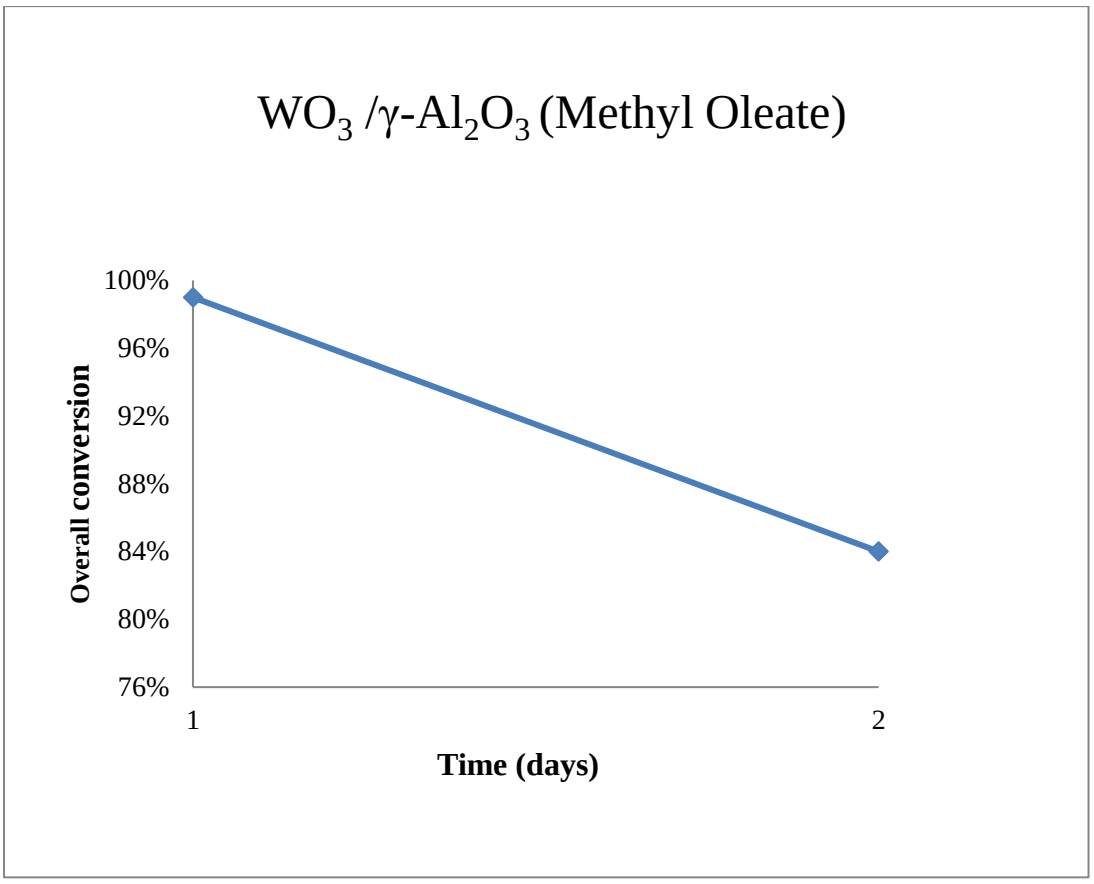

Fig. 4.Effect of continuous usage of catalyst on overall conversion.

Operating conditions: Reduction temperature: 300 ºC

Reaction temperature: 400 ºC and Hydrogen flowrate: 60 mL/min

4.8 XPS catalyst loading results

From the results of XPS of all the catalysts, it is found that $WO_3/\gamma\text{-}Al_2O_3$ catalyst also contains $Al_2(WO_4)_3$ which is responsible for cracking of hydrocarbon chain. Moreover, the oxide form of Ni present in Ni-$W/\gamma\text{-}Al_2O_3$ (oxide) is NiO which confirms Ni-W oxide is present as $NiWO_4/\gamma\text{-}Al_2O_3$. For the Ni-W sulfide catalyst, it is found that this catalyst also contains some traces of NiO because the precursor used to promote the W-sulfide catalyst had 'O' in it.

CHAPTER 5

CONCLUSIONS AND RECOMMENDATIONS

In this research, hydrotreating tungsten catalyst was used to study the hydrodeoxygenation reaction for production of green diesel from biodiesel. Effects of feedstock, pretreatment (reduction) temperature, reaction temperature, hydrogen flowrate, promoter, anion (oxide vs sulfide) and prolonged usage were tested. Pretreatment temperature is the most important parameter for green diesel selectivity and yield. It is concluded that pretreatment temperature of 300ºC-350ºC and reaction temperature of 400ºC is ideal for carrying out hydrodeoxgenation reaction with W catalyst because at 300ºC, C_{18}/C_{17} ratio is maximum but at reduction temperature of 350ºC, green diesel yield is maximum. It is found that at low reduction temperature (250ºC), hydrodeoxygenation is also favored along with decarbonylation and decarboxylation. At higher reduction temperatures (300ºC and 350ºC) more selectivity towards green diesel is achieved indicating only two reaction pathways i.e. decarbonylation and decarboxylation.

Addition of Ni increases the selectivity, yield and overall conversion thereby preventing the formation of lower hydrocarbons (C_{10}-C_{15}). It is found that overall conversion with oxide catalyst is a little more than sulfide catalyst (98.5% vs 92.4%). But the green diesel yield with sulfide catalyst is approximately 10 times more than oxide catalyst.

This is because WO_3 forms $Al_2(WO_3)_4$ with the alumina support which is also acidic in nature, and thereby cracks the hydrocarbon chain of the FAME and hence decreases the yields of green diesel (forming kerosene range hydrocarbons as shown in the Appendix A). But with sulfide catalyst, there is no interaction with the support so sulfide catalyst turns out to be more superior than oxide catalyst. Moreover, with Ni promoted sulfide catalyst ($NiWS_4$), the conversion is a little less than $NiWO_4$.

Recommendations

When using W catalyst for hydrodeoxgenation of biodiesel to produce green diesel, the ideal pretreatment (reduction) temperature should be about 300ºC-350ºC and reaction temperature should be 400ºC. Highest conversion (~ 100%), yields and selectivity for green diesel can be obtained when Ni is added to WS_2 catalyst. The precursor used for adding Ni must be devoid of O and other impurities and must only contain sulfide ions. If it desired to produce mixture of hydrocarbons (C_{10}-C_{19}) then WO_3 /γ-Al_2O_3 works best and if only green diesel is desired then $NiWS_4$ is the best catalyst according to this research. Future runs should include longer reaction times (10-12 h) to determine if activity of catalyst can be sustained to produce same level of conversion. Thus, Ni promoted W sulfide seems to be a promising catalyst for hydrodeoxgenation to produce green diesel from biodiesel in the near future.

REFRENCES

[1] E. Furimsky et al., Applied Catalysis A: General 199 (2000) 147–190.

[2] M. Mohammad et al. / Renewable and Sustainable Energy Reviews 22 (2013) 121–132.

[3] Y. Bie., J. Lehtonen. And J. Kanervo., Applied Catalysis A: General., 526., 2016., 183 – 190.

[4] I.E. Wachs et al. / Catalysis Today 116 (2006) 162–168.

[5] A. Gutierrez., E.M. Turpeinen., T.R. Viljava., O. Krause., Catalysis Today., 285., 2017., 125-134.

[6] O.B. Ayodele., H.U. Farouk., J. Mohammed., Y. Uemura and W.M.A.W. Daud., Journal of the Taiwan Institute of Chemical Engineers., 50., 2015., 142-152.

[7] A.E. Coumans., E.J.M Hensen., Applied Catalysis B: Environmental., 201., 2017., 290 – 301.

[8] Kung T. Ng and David M. Hercules., The Journal of Physical Chemistry, Vol. 80, No. 19, 2094 (1976).

[9] Y.K. Hong., D.W. Lee., H.J Eom., K.Y. Lee., Journal of Molecular Catalysis A: Chemical., 392., 2014., 241 – 246.

[10] P.A. Nikulshin., V.A. Salnikov., A.N. Varakin., and V.M. Kogan., Catalysis today 271., 2016., 45-55.

[11] B.P. Pattanaik., R.D. Misra., Renewable and Sustainable Energy reviews., 73., 2017., 545-557.

[12]. R. Thomas., E. M. Van Oers., V. H. J. DE Beer., J. Medema., and J. A. Moulijn., Journal of catalysis 76, 241-253 (1982).

[13] K. Jenistova., I. Hachemi., P.M. Arvela., N. Kumar., M. peurla., L. Capek., J. Warna., D.Y. Murzin., Chemical Engineering Journal., 316., 2017., 401-409.

[14] O.B. Ayodele., O. S. Togunwa., H. F. Abbas., W. M. W. Daud., Energy Conversion and Management., 88., 2014., 1104–1110.

[15] A.N. Varakina., V.A. Salnikova., M.S. Nikulshinaa., K.I. Maslakovb., A.V. Mozhaeva. and P.A. Nikulshina., Catalysis Today., 292., 2017., 110–120.

[16] I. Hachemi., N. Kumar., P.M. Arvela., J. Roine., M. Peurla., Jarl Hemming., J. Salonen., D.Y. Murzin., Journal of Catalysis., 347., 2017., 205–221.

[17] Deng, Y., *PhD.* dissertation, University of New Hampshire, 2017.

[18] O.B. Ayodele., H.F. Abbas., W.M.A.W. Daud., Energy Conversion and Management., 88., 2014., 1111–1119.

[19] H. Imaia., T. Kimuraa., K. Terasakaa., X. Lia., K. Sakashitaa, S. Asaoka., S.S. Al-Khattaf., Catalysis Today (2017), http://dx.doi.org/10.1016/j.cattod.2017.08.023.

[20] M. Gousi., C. Andriopouloua., K. Bourikasb., S. Ladasc., M. Sotirioub, C. Kordulisa., A. Lycourghiotisa., Applied Catalysis A: General 536., 2017., 45–56.

[21] E. Kordoulia., L. Sygelloub., C. Kordulisa., K. Bourikasc., A. Lycourghiotis., Applied Catalysis B: Environmental 209., 2017., 12–22.

[22] L. Zhou, A. Lawal., Applied Catalysis A: General., 532., 2017., 40–49.

[23] A.E. Coumans, E.J.M. Hensen., Catalysis Today., 298., 2017., 181–189.

[24] M. Wang, M. He, Y. Fang., J. Baeyensc., T. Tan., Catalysis Communications 100., 2017., 237–241.

[25] K. Kandel., J. W. Anderegg., N.C. Nelson., U. Chaudhary., I.I. Slowing., Journal of Catalysis 314 (2014) 142–148.

[26] V.N. Sapunov., A.A. Stepacheva., J. Wärnåc., P.M. Arvelac., B.D. Stein., D.Y. Murzin., V.G. Matveeva., Journal of Industrial and Engineering Chemistry 46., (2017) 426–435.

[27] P. Bui., J. Antonio., S.T. Oyama., A. Takagaki., A.I. Molina., H. Zhao., D. Li., E.R. Castellon., A.J. Lopez., Journal of Catalysis., 294., 2012., 184-198.

[28] C. Kordulis., K. Bourikas., M. Gousi., E. Kordouli., A. Lycourghiotis., Applied catalysis B: Environmental 181., 2016., 156-196.

[29] P.A. Nikulshin., P.P Minaev., A.V. Mozhaev., K.I. Maslakov., M.S. Kulikova and A.A. Pimerzin., Applied catalysis B: Environmental 176-177., 2015., 374-384.

[30] S. T. Oyama, X. Wang, F. G. Requejo, T. Sato and Y. Yoshimura, Journal of Catalysis., 209., 2002., 1 – 5.

[31] S. Echeandia, P.L. Arias., V.L. Barrio, B. Pawelec and J.L.G. Fierro., Applied Catalysis B: Environmental., 101., 2010., 1–12.

[32] Thangaraju M. Sankaranarayanan., Antonio Berenguer., Catalysis Today., 243., 2015., 163–172.

[33] E. Rodrı´guez-Castello´., A. Jime´nez-Lo´pez and D. Eliche-Quesad.,
Fuel 87., 2008., 1195–1206.

[34] Juan Arturo Mendoza-Nieto, Oscar Vera-Vallejo., Luis Escobar-Alarcón., Dora Solís-Casados., Tatiana Klimov., Fuel., 110., 2013., 268–277.

[35] S.K. Hoekman., A. Broch., C. Robbins., E. Ceniceros., M. Natarajan., Renewable and Sustainable Energy Reviews., 16., 2012., 143-169.

APPENDIX A

Product peaks at different reduction temperatures

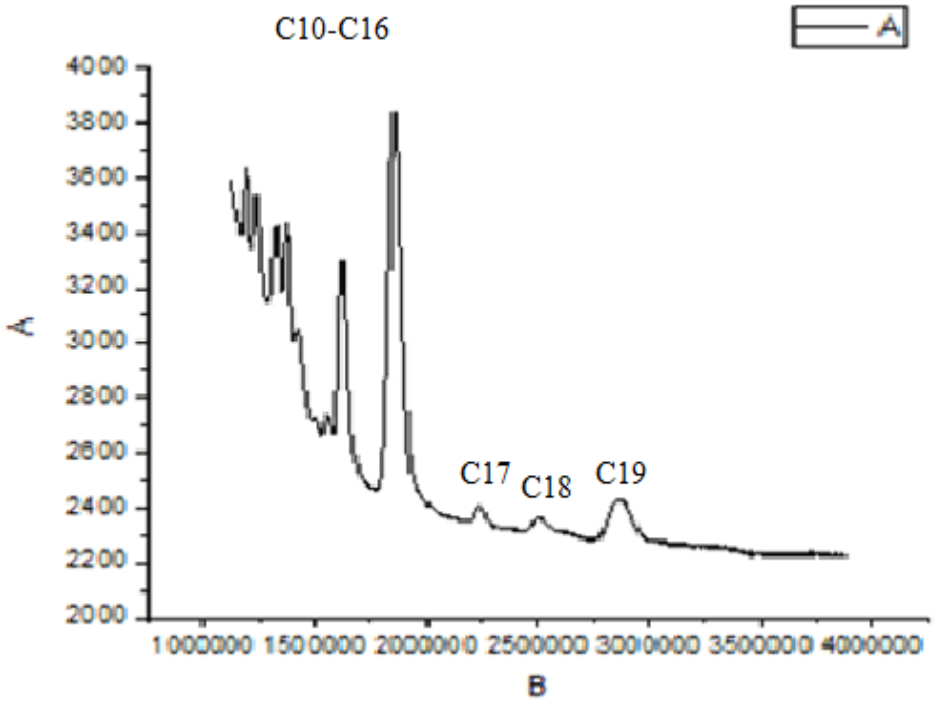

Product peaks at reduction temperature of 250 ºC. Catalyst: WO_3 /γ-Al_2O_3.

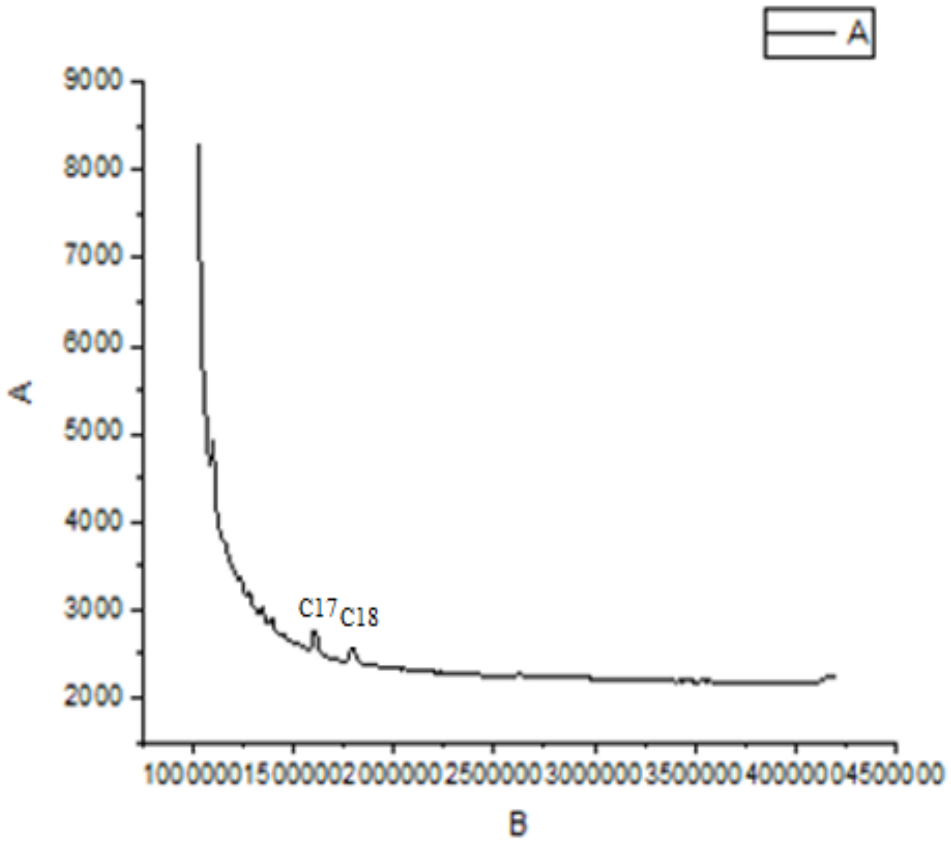

Product peaks at reduction temperature of 300 ºC. Catalyst: WO_3 /γ-Al_2O_3.

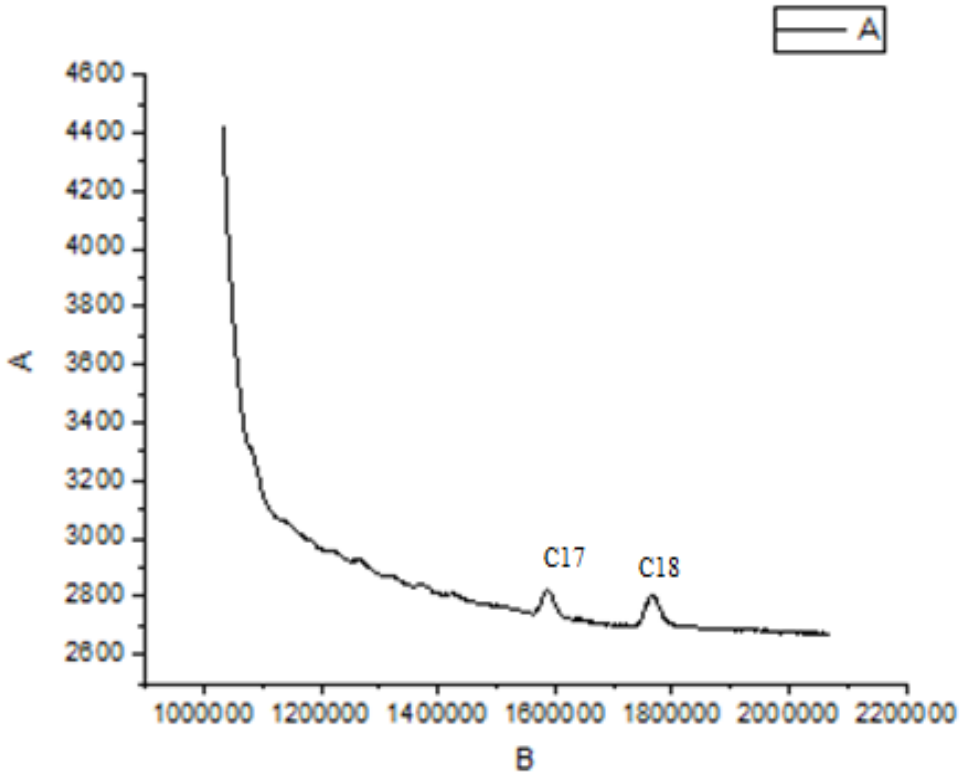

Product peaks at reduction temperature of 350 ºC. Catalyst: WO_3 /γ-Al_2O_3.

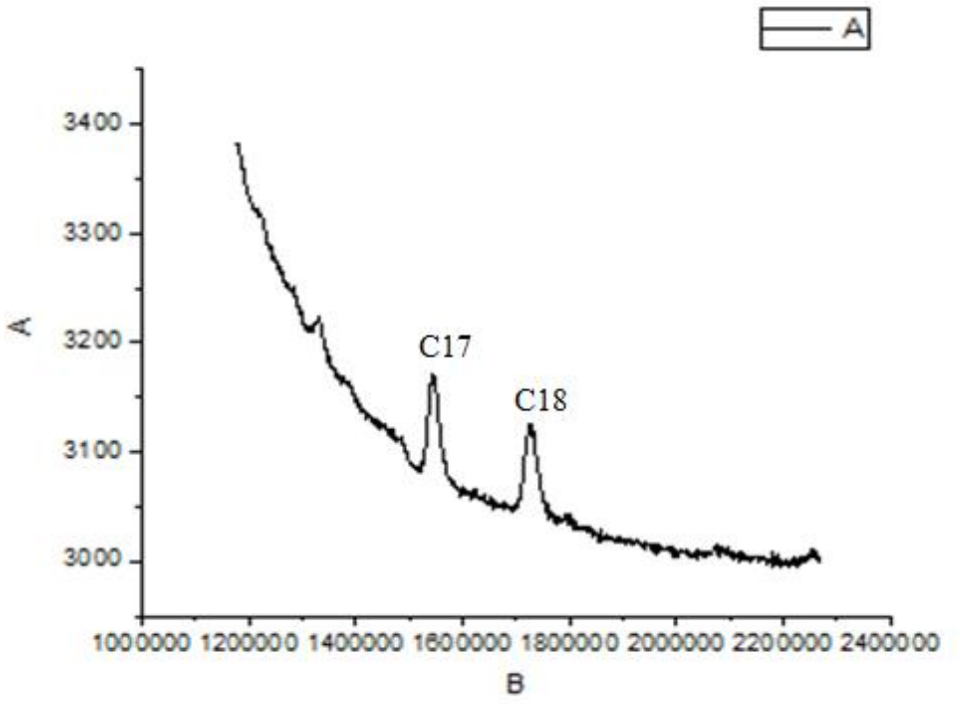

Product peaks at reduction temperature of 400 ºC. Catalyst: WO_3 /γ-Al_2O_3.

APPENDIX B

GC Calibration Curves

Calibration curves were prepared as follows:

20 μl of sample to be calibrated was added into 2 ml *iso*-octane to get the "specimen 0". After adequate shaking of specimen 0, 0.8 ml mixture was extracted and mixed with 1 ml *iso*-octane to get the "specimen 1". 1 ml of mixture specimen 1 was extracted and mixed with 1ml *iso*- octane to get "specimen 2". 1 ml of mixture was extracted from specimen 2 and mixed with 1 ml *iso*-octane to get "specimen 3"; (v) 1 ml of mixture was extracted from specimen 3 and mixed with 1 ml *iso*-octane to get "specimen 4."

Except the specimen 0, the mass concentration of specimen 1-4 was calculated by Equation:

$$W_i = \frac{(W_{i-1})(m_i)}{(m_i)(1-W_{i-1}) + I_i}$$

W_i (g/g) and W_{i-1} (g/g) is the mass concentration of specimen i and specimen i-1, respectively

m_i (g) is the weight of mixture extracted from specimen i-1

I_i (g) is the weight of *iso*-octane added to the mixture, while concentration of specimen 0 is calculated by weight of methyl oleate divided by added *iso*-octane.

3 μl samples of specimen 1-4 were extracted and test by GC machine. Software *Origin* was used for calculating the area of peaks. Finally, these area values were correlated with the corresponding the mass concentration to the calibration curve as shown below.

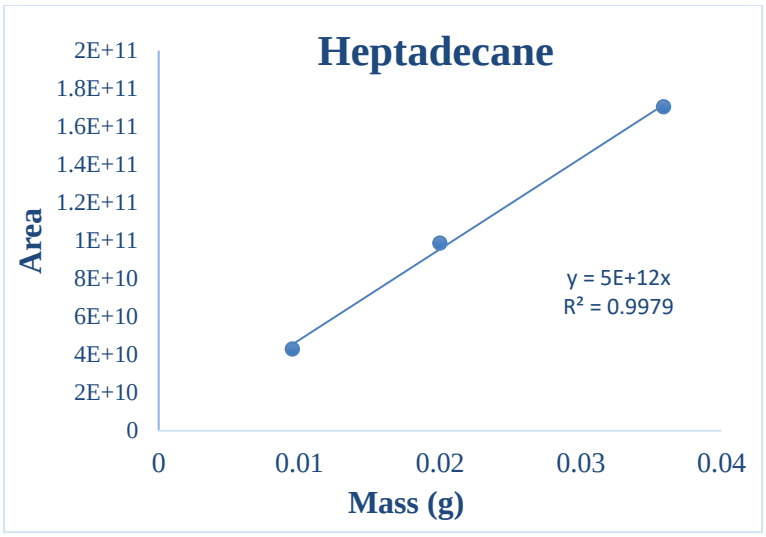
Heptadecane
2E+11
1.8E+11
1.6E+11
1.4E+11
1.2E+11
1E+11
8E+10
6E+10
4E+10
2E+10
0
Area
y = 5E+12x
R² = 0.9979
0
0.01
0.02
0.03
0.04
Mass (g)

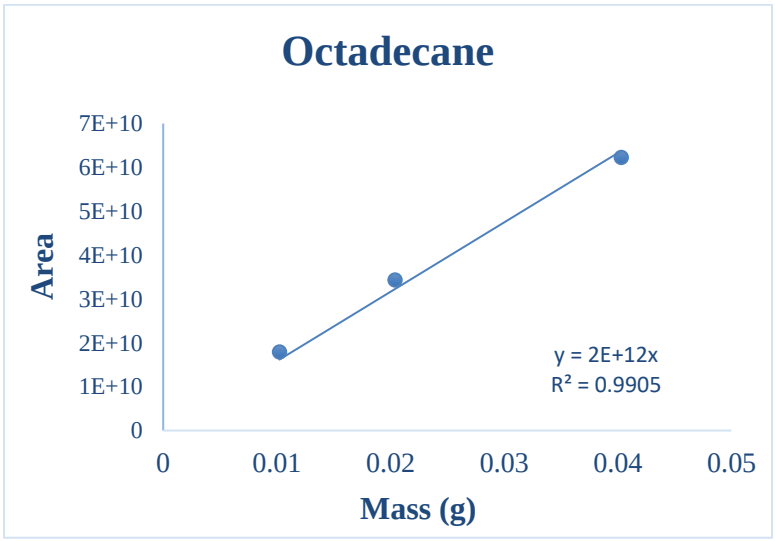
Octadecane
7E+10
6E+10
5E+10
4E+10
3E+10
2E+10
1E+10
0
Area
y = 2E+12x
R² = 0.9905
0
0.01
0.02
0.03
0.04
0.05
Mass (g)

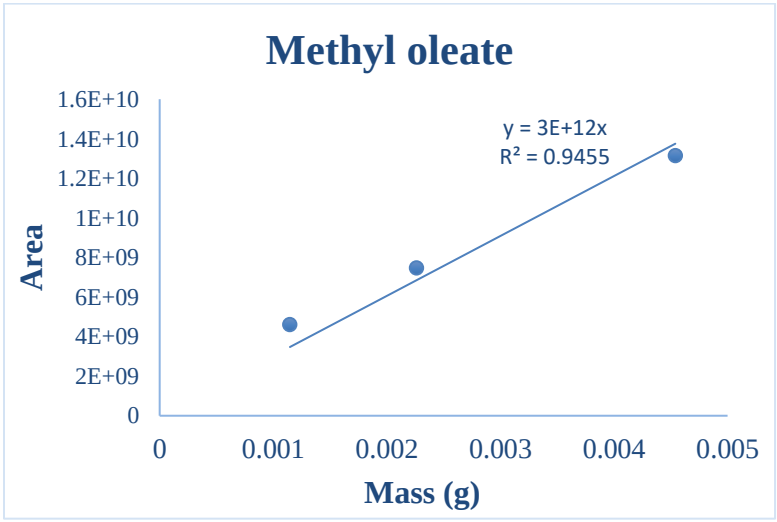
Methyl oleate
1.6E+10
1.4E+10
1.2E+10
1E+10
8E+09
6E+09
4E+09
2E+09
0
Area
y = 3E+12x
R² = 0.9455
0
0.001
0.002
0.003
0.004
0.005
Mass (g)

APPENDIX C

CALCULATION OF BIODIESEL CONVERSION AND GREEN DIESEL YIELD

3 mL of gas sample from the bubbler outlet or reactor outlet was injected into the GC via a 5 mL pressure-lock syringe. The resulting curve was designated as FAME inlet and outlet, as well as heptadecane and octadecane outlet. The area of peaks was integrated by *OriginPro*. A sample calculation of green diesel conversion is shown below:

- FAME inlet GC area = 2.3763×10^{8}
- FAME outlet GC area = 8.3049×10^{6}
- Heptadecane GC area = 1.988×10^{6}
- Octadecane GC area = 3.323×10^{6}
- Calibration cure slope of FAME = 3×10^{12}
- Calibration cure slope of heptadecane = 5×10^{12}
- Calibration cure slope of octadecane = 2×10^{12}
- FAME inlet mass = $(2.3763 \times 10^{8})/(3 \times 10^{12}) = 7.921 \times 10^{-5}$ g

- FAME outlet mass = $(8.3049 \times 10^{6})/(3 \times 10^{12}) = 2.7683 \times 10^{-6}$ g
- Heptadecane outlet mass = $(1.988 \times 10^{6})/(5 \times 10^{12}) = 3.976 \times 10^{-7}$ g
- Octadecane outlet mass = $(3.323 \times 10^{6})*(2 \times 10^{12}) = 1.6616 \times 10^{-6}$ g

Overall green diesel conversion = [(FAME inlet mass) - (FAME outlet mass)] / (FAME inlet mass) = $[(7.921 \times 10^{-5}\ g) - (2.7683 \times 10^{-6}\ g)] / (7.921 \times 10^{-5}\ g) =$ 96.5%

C_{18}/C_{17} Ratio = (Octadecane outlet mass) / (Heptadecane outlet mass) = $(1.6616 \times 10^{-6}\ g) / (3.976 \times 10^{-7}\ g) = 4.18$.